

This work has been submitted to the IEEE for possible publication. Copyright may be transferred without notice, after which this version may no longer be accessible.

Compositional Semantics for Open Vocabulary Spatio-semantic Representations

Robin Karlsson¹, Francisco Lepe-Salazar², Kazuya Takeda^{1,3}

Abstract—General-purpose mobile robots need to complete tasks without exact human instructions. Large language models (LLMs) is a promising direction for realizing commonsense world knowledge and reasoning-based planning. Vision-language models (VLMs) transform environment percepts into vision-language semantics interpretable by LLMs. However, completing complex tasks often requires reasoning about information beyond what is currently perceived. We propose latent compositional semantic embeddings z^* as a principled learning-based knowledge representation for queryable spatio-semantic memories. We mathematically prove that z^* can always be found, and the optimal z^* is the centroid for any set \mathcal{Z} . We derive a probabilistic bound for estimating separability of related and unrelated semantics. We prove that z^* is discoverable from visual appearance and singular descriptions by iterative gradient descent optimization. We experimentally verify our findings on four embedding spaces incl. CLIP and SBERT. Our results show that z^* can represent up to 10 semantics encoded by SBERT, and up to 100 semantics for ideal uniformly distributed high-dimensional embeddings. We demonstrate that a simple dense VLM trained on the COCO-Stuff dataset can learn z^* for 181 overlapping semantics by 42.23 mIoU, while improving conventional non-overlapping open-vocabulary segmentation performance by +3.48 mIoU compared with a popular SOTA model.

Index Terms—Open-vocabulary segmentation, learned knowledge representation, object discovery, compositional semantics

I. INTRODUCTION

General-purpose mobile robots promise machines capable of safely completing tasks in novel environments without relying on exact human programmed instructions. A promising approach to realize general-purpose robots is to leverage large language models (LLMs) [1]–[9] trained on internet scale information about the world. LLMs compliment the weaknesses of conventional human programmed robots by enabling weakly specified goal definitions in natural language [1], hierarchical planning by program synthesis [6]–[8], and reasoning with commonsense knowledge [9].

The world knowledge and planning capabilities of LLMs is grounded in the external environment by aligned multi-modal vision-language models (VLMs) [10]–[20]. VLMs transform sensor percepts into an open set of semantic vision-language (VL) embeddings that are interpretable by similarity with other natural language embeddings. LLMs are thus able to receive and query information about the environment by words and

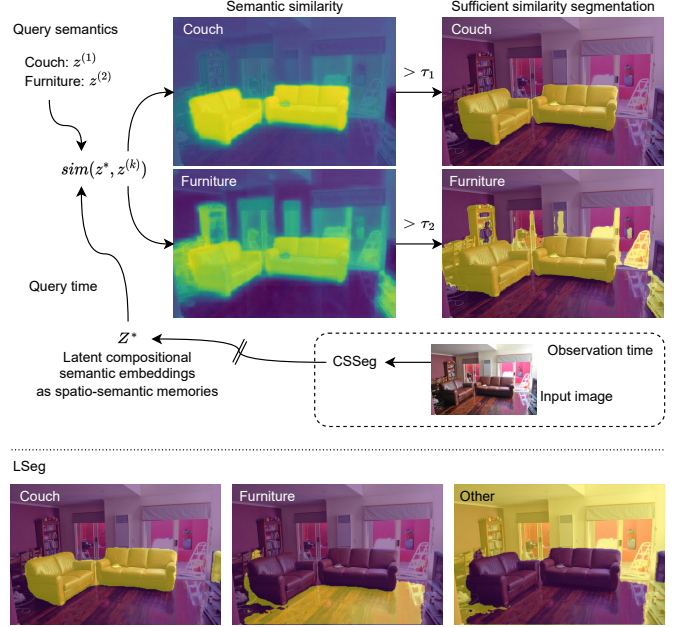


Fig. 1. Our unconditional compositional semantic segmentation (CSSeg) dense VLM model maps an image into a latent compositional semantic embedding map Z^* at observation time. Any semantics $z^{(k)}$ can be queried by similarity with z^* without requiring original input images. z^* is learned from non-overlapping semantic segmentation data. Boolean segmentation masks are obtained by learned sufficient similarity threshold values τ_k . Conventional unconditional models like LSeg [10] fail at inferring semantic overlap (*couch* is also *furniture*) and incomplete partitionings (*other* is a flawed substitute for unspecified semantics). Projecting Z^* to spatial coordinates result in accurate and rich open-vocabulary spatio-semantic memories.

sentences using VLMs as an interface. The predicted semantic embeddings need to be spatially grounded into spatio-semantic representations for precise spatial comprehension and reasoning [2], [21], [22]. Spatial grounding of VL embeddings in 3D can be done by projecting 2D dense VL embedding maps to point clouds [23]–[25] or neural radiance fields (NeRF) [26].

Completing tasks generally requires information beyond what is currently observed. A spatio-semantic cognitive memory [27], or semantic scene representations [28], enables a mobile robot to query semantic information about prior observations [23]–[25], to navigate [21], and do planning by language-based reasoning [9]. Common spatio-semantic representations for mobile robots are 3D reconstruction [29], object-centric, topological maps [30], scene graphs [31], and top-down metric grid maps [32].

The spatio-semantic environment representation for general-purpose mobile robots needs to satisfy three properties: First, the representation needs to encode rich open-set semantic object descriptions [33]–[35]. For narrow problems like object

Manuscript received October 4, 2023

This work was supported by JST SPRING, Grant Number JPMJSP212.

¹Robin Karlsson and Kazuya Takeda are with the Graduate School of Informatics, Nagoya University, Japan (karlsson.robin@g.sp.m.is.nagoya-u.ac.jp)

²Francisco Lepe-Salazar is with Ludolab, México (flepe@ludolab.org).

³Kazuya Takeda is also with TIER IV, Japan (kazuya.takeda@tier4.jp).

Code will be publicly available upon acceptance

avoidance in constrained environments, it may suffice to detect and represent an object by one of a fixed set of classes like *table*. A general-purpose agent [9] however, requires a richer compositional representation of the object including alternative names like *desk*, properties like *rigid*, and affordances like *flat surface*, all of which cannot be manually annotated during the system development phase. Secondly, the representation needs to support querying of overlapping semantics, such as a *dog* also being an *animal*. Overlapping semantics must be learnable from independent observations or datasets without relying on human customization effort limiting scalability [36]. Third, the representation must be efficient in terms of storage. Spatio-temporal accumulations of raw observations rapidly grow into an unreasonable amount of data [28]. To keep the environment representation compact, observations need to be abstracted into declarative semantic memories [35], [37], [38]. An additional practically beneficial property is explicit environmental representation. Explicit representations can communicate to humans robots’ environmental understanding, intended plan of actions, along with interpretable factors for decision making. Explicit representations also allow humans to provide precise spatially grounded instructions to robots.

In this paper, we investigate latent compositional semantics as a means to compactly represent objects by rich semantic descriptions within explicit environment representations. We prove that mathematical properties of high-dimensional hyperspheres enable a single compositional semantic embedding z^* to define a set of semantic text descriptions encoded into semantic embeddings $\mathcal{Z} = \{z^{(1)}, z^{(K)}\}$. Our experiments verify that a single embedding z^* can robustly represent 10 semantically related real-world embedded text descriptions, and up to 100 randomly sampled embeddings for ideal uniformly distributed embedding spaces. Based on our findings, we propose a new perspective on unconditioned dense VL embedding prediction models [10] as a scalable, robust, and learnable neural approximations of semantic networks [39] for knowledge representation.

Our idea of latent compositional semantics has strong support in cognitive psychology, neuroimaging, and philosophy. Cognitive scientists believe there exist two types of long-term memory: declarative and nondeclarative [35]. Declarative memory involves the conscious recollection of events and facts, encompassing memories that can be explicitly articulated or recounted, while also including those that elude verbal description. It is also known as explicit memory. Declarative memory is further divided into two primary forms: episodic memory, which concerns personal experiences and specific events in particular places and times, and semantic memory, which encompasses general knowledge about the world, concepts, and language [35]. Semantic memories are derived from an agent’s experiences but is characterized by its abstract and conceptual nature, devoid of ties to any specific encounter [38]. Our approach implements the idea of semantic memories into a computational learning framework.

Semantic concepts are organized into hierarchies [35]. These hierarchies comprise three levels: super-ordinate categories, situated at the top (e.g., items of furniture); basic-level categories, positioned in the middle (e.g., chair); and

subordinate categories at the bottom (e.g., office chair) [37]. Concepts are rarely processed in isolation; instead, the processing is heavily influenced by the current context and environment [33], [34]. Qualities of observable objects are easier to contemplate [35], underscoring the intricate nature of how perceptual and cognitive systems interact when processing concepts and information about the world. Our work shows how machines can learn hierarchical concepts from independent visual observations.

Philosophers argue that real world objects are generally not perfectly described by a single category, as categories themselves are not precisely specifiable. Categories with fuzzy boundaries are called natural kinds. To give an example, finding a perfect logical specification of a platonic “chair” is futile and is bound to result in unintended inferences [40]. Representing real world objects instead in terms of fuzzy semantic descriptions, and determining semantic membership through similarity, has strong support in philosophy. Wittgenstein [41] proposes that members of a category share family resemblance instead of necessary and sufficient characteristics. Lakoff [42] argues for categorization based on prototype similarity and analogies. Schwartz [43] writes that category membership is a matter of degree, meaning similarity to a cluster prototype is a useful measure of membership. In this work, we provide a computational framework to learn natural kinds from incomplete object descriptions.

Our contributions are three-fold:

- A mathematical analysis proving that latent compositional semantic embeddings z^* is a principled representation for rich object descriptions by a set of semantics \mathcal{Z} . The optimal z^* for \mathcal{Z} is simply the centroid of \mathcal{Z} and does not require contrastive learning.
- An empirical investigation of four VL embedding spaces in terms of uniformity, alignment, and their capacity to represent compositional semantics by z^* .
- Experiments proving z^* are discoverable from visual appearance and singular descriptions by training unconditional dense VLMs and queried by sufficient similarity.

The rest of the paper is organized as follows. Section II explains how compositional semantics connects several fields of artificial intelligence. In Sec. III we introduce compositional semantics and mathematical properties. A brief presentation of dense VLMs used for inferring compositional semantics from observations is given in Sec. IV. We explain experiments and results in Sec. V-VI. We summarize our findings in Sec. VII.

II. BACKGROUND AND RELATED WORKS

Knowledge representation. A general-purpose intelligent agent needs to store information about the world in a practically useful form for reasoning and task completions. This problem is called knowledge representations. An ontology is a framework for organizing and representing knowledge into a hierarchy of categories or concepts. Philosophers and artificial intelligence scientists commonly recognize six types of knowledge [44]: concrete objects including things and stuff, abstract categories for organizing objects in terms of similarity by shared properties, measurements for ordering

of properties, and events, fluents, and time points specify temporally changeable statements.

First-order logic (FOL) [45] and extensions like fuzzy [46] and modal logic [47] traditionally express an object x being a member of a category *Category* as $Category(x)$ or $x \in Category$. Semantic networks [39] is a subset of FOL designed to represent knowledge as a directed graph of objects and categories. Objects are associated to one or more categories by $MemberOf(\cdot, \cdot)$ relations. Categories are associated to other categories to form a taxonomic hierarchy. The hierarchy of categories allows objects to inherit semantic descriptions from higher-level categories, implying that an object that is a chicken is also a bird (but not the other way):

$$Chicken(x) \Rightarrow Bird(x). \quad (1)$$

Frames [48] extend Semantic networks with inheritable default attribute values like $height = 1$ and properties $CanFly = True$ similar to object-oriented programming.

Semantic networks have several practical limitations. First, semantic vagueness is an inherent aspect of object descriptions as explained in Sec. I. Expressing degree of membership is challenging in purely logical representations. Secondly, the problem of inferring correct and diverse category associations from perception on real world system is not addressed. Finally, a complete ontology encompassing the entire world does not exist. A scalable method for learning and revising a diverse set of category associations from incomplete and noisy data is needed.

We propose compositional semantic embeddings as a principled and scalable learning-based approach to obtain compact and semantically diverse object descriptions from uncurated data.

Natural language processing. The study of using natural language as an interface for human-machine communication, and how to enable machines to leverage human written knowledge, is called natural language processing (NLP). Natural language is ambiguous and sentence correctness is not perfectly decidable by rules [44]. Language models (LM) [49], [50] instead learn to predict the likelihood $p(\mathcal{X})$ of any sequence of text tokens \mathcal{X} according to a natural language dataset.

Word embeddings [51], [52] substitute non-semantic word tokens by a semantic vector representing the meaning of the word. Word embeddings are discovered from maximizing similarity of embeddings of co-occurring words [53]. Contextual representations [54] extends word embeddings by encoding context from surrounding words. Large language models (LLM) [49], [50], [55] can generate semantic embeddings out of entire sentences. Our approach differs from word and sentence embeddings as we represent a set of semantic embeddings representing an object description by a single compositional semantic embedding.

Clustering [56] and mixture models [57], [58] in NLP discover groups of semantically similar text data. The Latent Dirichlet Allocation (LDA) model [57] parses documents into mixtures of discovered latent topics that allow a finer semantic similarity search. A generative probabilistic mixture model $p(z)$ approximates the distributions of semantic embeddings

$z \in \mathcal{Z}$ by K mixture components $p_k(z)$ weighted by the probability π_k that each mixture component is sampled

$$p(z) = \sum_{k=1}^K \pi_k p_k(z). \quad (2)$$

The optimal model is a mixture of Dirac delta distributions $p_k(z) = \delta(z - z^{(k)})$ with number of mixtures K equaling the number of semantics in the distribution \mathcal{Z} . As the set of possible semantics in natural languages are unbounded, a common distribution approximation is the Gaussian mixture model (GMM) with $K \ll |\mathcal{Z}|$ Gaussian components $p_k(z) = \mathcal{N}(\mu_k, \Sigma_k)$ representing the K best semantic clusters. However, this approximation has practical limitations. The required maximum clusters K is generally not known. Optimizing the mixture model $p(z)$ is challenging. Storing the the mixture distribution parameters or all K semantic embeddings μ_k can be inefficient.

Our compositional semantics approach instead leverage properties of high-dimensional hyperspheres to find an optimal semantic embedding z^* akin to clustering. The vector z^* defines $p(z \in \mathcal{Z})$ by similarity instead of approximating the entire distribution $p(z)$ as mixture models do. Our approach has mathematical guarantees of optimality, and can represent a large set of semantics by a single embedding while optimizable by gradient descent.

Vision-language modeling. Multimodal models that semantically interpret images and text by a unified embedding space are called vision-language models (VLMs). Global description generating VLMs [11] consist of a visual $Enc_V()$ and language encoder $Enc_L()$. Both encoders are co-trained to generate a semantically similar visual and text embedding z_v and z_t for an input image x and text t in an aligned embedding space Z . Alignment enables VLMs to be used as an interface to query or express contents of visual data in natural language. Semantic correspondence between z_v and z_l is measured by cosine similarity. The encoders are typically trained on internet-scale image captioning datasets using contrastive learning. Global description models have many usages like image-text matching, multimodal search, multimodal generative modeling [59], and visual-question-answering [60]. However, outputs are not spatially grounded in the input image and therefore have limitations for tasks requiring precise spatial information such as navigation [2], manipulation [1], and mapping [21].

Dense description VLMs [10], [13]–[20] generate aligned embeddings for every image pixel for fitting semantics to object boundaries. MaskCLIP [16] aims to leverage the strong generalization power of global description VLMs by removing the global pooling layer. However, the output is considerably noisy and have limited practical usefulness for robotics tasks.

One approach to generate dense descriptions is to use an off-the-shelf region proposal (RP) model [61]. The RP model predicts a set of object crops that are interpreted by a global VLM [14]. The resulting global embedding is projected onto all pixels covered by the region. The object crop approach works well for object-centered image inputs typical for indoor robotics environments, but less so for large and

complex scenes requiring multi-scale object perception [20], [62]. Computational cost is high due to performing inference for every region separately.

Another direction of work instead trains a new vision model $f_\theta(\cdot)$ with an architecture and optimization scheme designed for dense feature representation. LERF [63] grounds language embeddings in a neural radiance field (NeRF) [64], allowing querying semantics in 3D environment representations. Open-vocabulary object detectors localize predicted VL embeddings to bounding boxes [65]. Works related to open-vocabulary semantic segmentation can be categorized into two types. Conditional OV semantic segmentation models [15], [19], [66], [67] allows fine-grained query guided by additional text and/or image input. One drawback is that conditional inference require the original image. Unconditional methods [10], [13], [18] learns to predict general embedding maps such that the likelihood is maximized over the training dataset. Contrary to global embedding models [11], unconditional semantic segmentation models are trained on relatively small densely annotated datasets. The expressiveness of unconditionally predicted embeddings is not yet deeply understood.

In this paper we present an interpretation of unconditional semantic segmentation predictions as latent compositional semantic embeddings z^* . We show that the representation z^* combines the compactness of unconditional inference, the expressiveness of conditional inference, and potentially the generality of global description VLMs.

Spatio-semantic representations. Mobile robots typically perform planning for spatial tasks by localizing its pose within a map [68]. ICP [69] or SLAM [70] by modern implementations [71]–[73] is the conventional approach to map 3D environments by matching sequential point clouds and accumulating them into a common vector space. Semantic SLAM not only estimate the geometry but also the semantics of the environment or an object [74] or segmentation level [75]. The 3D representation can be projected onto a 2D birds-eye-view (BEV) map convenient for navigation tasks [76]. The image-like 2D map representation is suitable for predictive generative modeling [32]. Until recently, semantic mapping approaches were limited to predefined sets of semantic classes, and thus to narrow tasks.

Open-vocabulary spatial representation methods encode maps by VL embeddings instead of class embeddings. The VL embeddings are typically generated by a pretrained global VLM [25], open-vocabulary object detector [22], or a dense VLM [21], [23], [24]. The open-vocabulary approach in principle allows querying any task-relevant semantics stored in the VL embeddings measuring cosine similarity with a text query embedding. NeRFs implicitly represents 3D objects and environments by a neural network [64], [77], [78] and have recently been extended represent open-vocabulary semantics [26]. Integrating LLMs opens up new possibilities for spatio-semantic reasoning based on a top-down perceptual feedback loop [22], [79] similar to the human vision-for-perception system [80]–[82].

Our work presents an interpretation of VL embeddings learned by dense open-vocabulary models as latent compositional semantic embeddings z^* . We show that z^* can combine

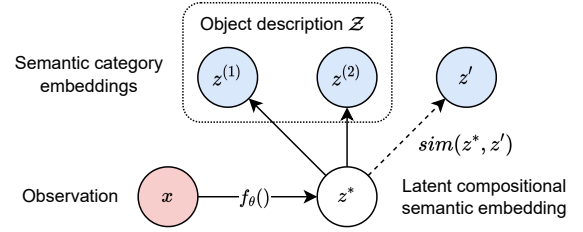


Fig. 2. The compositional semantics framework. An observation x is mapped into an embedding z^* that specifies an object description \mathcal{Z} in terms of interpretable semantic categories $z^{(k)}$ through fuzzy membership by similarity.

the generality of global description VLMs like CLIP [11] with the accuracy of dense VLMs like LSeg [10].

III. COMPOSITIONAL SEMANTICS

In this section, we first present the idea of compositional semantics, and how a single vector $z^* \in \mathbb{R}^D$ implicitly represents a diverse set of semantic object descriptions \mathcal{Z} . In Sec. III-B-III-C we derive properties of compositional semantic embeddings z^* for uniform and non-uniform embedding distributions based on mathematical analysis of high-dimensional hyperspheres. Finally, in Sec. III-D we analyze practical discoverability of compositional semantics in real world VL embeddings spaces by iterative gradient descent.

A. Compositional object representations

Knowledge representations aim to describe concrete objects by membership to abstract semantic categories. Semantic networks are a common object description representation encumbered by practical limitations. We propose compositional semantics as an efficient and practical vector space representation for describing objects by a potentially large set of semantic categories by a scaleable learning-based method. Compositionality means that complex expressions, such as sentences or functions, can be determined or understood based on the meanings of their individual parts [83].

Our proposed framework for compositional semantics is shown in Fig. 2. The objective is to find a hyperspherical latent compositional semantic embedding $z^* \in S^{D-1}$ for an object which is similar to all semantic embeddings in the set $\mathcal{Z} = \{z^{(1)}, \dots, z^{(K)}\}$ that broadly describe the object (see Sec. I). Semantic similarity is defined in terms of separation distance in the embedding space S^{D-1} . Distances between embeddings on unit hyperspheres in Euclidean vector spaces are conveniently represented by cosine similarity

$$\cos \omega = \frac{\langle z^*, z^{(k)} \rangle}{\|z^*\| \|z^{(k)}\|} = (z^*)^T z^{(k)}. \quad (3)$$

An observation x is mapped into a compositional semantic embedding z^* discovered by a learned one-to-one mapping function $f_\theta(x)$. The optimal embedding z^* is found by maximizing the mean cosine similarity (3) over all describing semantics $z \in \mathcal{Z}$. We presume the distribution $p(z)$ is approximate uniformly distributed. In this paper we show that contrastive optimization by minimizing (3) over negative samples z' is not required if \mathcal{Z} is known. The mathematical properties of high-dimensional hyperspheres ensure that any

other randomly sampled embeddings is very likely to be dissimilar to z^* . The optimal compositional semantic embedding z^* thus separates the set of describing semantics \mathcal{Z} from all other semantics $z' \sim U(S^{D-1})$. Observations x denote any observable representation including image pixel regions.

During inference, the representation z^* for an observation x , implicitly encodes $\mathcal{Z} = \{z^{(1)}, \dots, z^{(T)}\}$ concatenated from past independent learning samples $(x^{(t)}, z^{(t)})$. From the perspective of knowledge representation, z^* implicitly encodes the degree of membership for any queried semantic z by semantic distance or equivalently cosine similarity (3) :

$$\text{MemberOf}(x, z) \propto \text{sim}(z^*, z) \quad z^* := f_\theta(x). \quad (4)$$

The set of inferred $\hat{\mathcal{M}}$ and original \mathcal{M} set of object descriptions are approximately equal

$$\hat{\mathcal{M}} = \{\text{MemberOf}(x, \hat{z}) \mid \hat{z} \in \hat{\mathcal{Z}}\} \quad (5)$$

$$\mathcal{M} = \{\text{MemberOf}(x, z) \mid z \in \mathcal{Z}\} \quad (6)$$

$$|\hat{\mathcal{M}} \cup \mathcal{M}| \simeq |\mathcal{M}| \quad (7)$$

as the set of inferred sufficiently similar semantic description embeddings are approximately equal

$$\hat{\mathcal{Z}} = \{\hat{z} \mid \text{sim}(z^*, \hat{z}) > \tau \quad \forall \hat{z} \in S^{D-1}\} \simeq \mathcal{Z}. \quad (8)$$

The degree of membership by similarity (4) reflects the fact that real world objects rarely have a single, clear-cut semantic specification [41], [42]. The threshold of sufficient semantic membership τ is subjective and needs to be optimized in respect to a purpose or task [43]. Note that the mapping $f_\theta(x)$ discovers z^* from independent samples $(x^{(t)}, z^{(t)})$ by iterative gradient descent.

B. Compositional properties for uniform distributions

VL embeddings are typically located on the surface of a high-dimensional unit hypersphere. In this section we analyse the compositional properties of VL embeddings spaces based on mathematics for high-dimensional probability distributions [84]. We begin the analysis by formally defining latent compositional semantic embeddings z^* .

Definition 1. A vector $z^* \in \mathbb{R}^D$ on the unit hypersphere S^{D-1} is a compositional semantic embedding for a set of semantic embeddings $z \in \mathcal{Z}$ if

$$\mathbb{E} \text{sim}(z^*, z) > \mathbb{E} \text{sim}(z^*, z') \quad \forall z \in \mathcal{Z}, z' \sim U(S^{D-1}) \quad (9)$$

where $U(S^{D-1})$ is the uniform distribution over S^{D-1} .

The following theorem specify the theoretically optimal z^* embedding is simply a centroid.

Theorem 1. [Discoverability I] It is always possible to find the optimal compositional semantic embedding $z^* \in \mathbb{R}^{D \gg 1}$ satisfying Definition 1 as the centroid of the set of semantics \mathcal{Z}

$$z^* = \frac{1}{K} \sum_{i=1}^K z^{(i)} \quad \forall z^{(i)} \in \mathcal{Z}. \quad (10)$$

Proof. See Appendix A. \square

The proof is based on finding the z^* maximizing cosine similarity by partially differentiating the equivalent minimum square distance.

A property of high-dimensional vector spaces is that any two random variable vectors are expected to be approximately orthogonal. The following lemma is used to prove Theorem 1

Lemma 1. [Expected similarity] For two independent random vectors $Z^{(i)}, Z^{(j)}$ sampled from an isotropic high-dimensional distribution $Z \in \mathbb{R}^D$ with $D \gg 1$

$$\mathbb{E} \text{sim}(Z^{(i)}, Z^{(j)}) = \frac{1}{\sqrt{D}}. \quad (11)$$

Proof. See Appendix B. \square

The proof involves recognizing Z as an isotropic distribution and computing the expectation of a dot product for two random vectors $Z^{(i)}$ and $Z^{(j)}$.

Next we derive a probabilistic bound defining the separability of a set \mathcal{Z} of object descriptions and random descriptions z' by similarity with the latent compositional semantic embedding z^* for \mathcal{Z} .

Theorem 2. [Probabilistic bound] The probability P a compositional semantic embedding z^* is more similar to all its semantic members $z \in \mathcal{Z}$ than any unrelated semantic embedding $z' \sim U(S^{D-1})$ is

$$P(\text{sim}(z^*, z) > \text{sim}(z^*, z')) = 1 - \frac{1}{2} I_{\sin^2(\theta_{min})} \left(\frac{D-1}{2}, \frac{1}{2} \right) \quad (12)$$

where $I_x(a, b)$ is the regularized incomplete beta function and

$$\theta_{min} = \arccos(\text{sim}(z^*, z_{min})) \quad (13)$$

is the angle θ_{min} defined by the least similar member

$$z_{min} = \arg \min(\text{sim}(z^*, z)) \quad \forall z \in \mathcal{Z}. \quad (14)$$

Proof. See Appendix C. \square

The proof is based on noting that the probability P a randomly sampled unrelated embedding z' falsely in the set of semantic members \mathcal{Z} is proportional to the area ratio of the hyperspherical cap S_{cap}^{D-1} spanned by z^* and z_{min} . The proof builds upon Lemma 1 and 2.

Lemma 2. [Hyperspherical cap] The compositional semantic embedding z^* and all semantic member embeddings $z \in \mathcal{Z}$ lie in a hyperspherical cap S_{cap}^{D-1}

$$\{z^*\} \cup \mathcal{Z} \in S_{cap}^{D-1} = \{z \in \mathbb{R}^D : \|z\| = 1, \theta_z \leq \theta_{min}\}. \quad (15)$$

Proof. See Appendix D. \square

We conclude that latent compositional semantic embeddings z^* can always be found for VL embeddings. The goodness of z^* can be measured by the probabilistic estimate (12)

C. Compositional properties for non-uniform distributions

The mathematical properties for latent compositional semantic embeddings z^* in Sec. III-B are derived for uniformly distributed embeddings. In this section, we analyze the validity of the results for non-uniform hyperspherical distributions.

Proposition 1 (Discoverability II). *It is always possible to find an optimal compositional semantic embedding $z^* \in \mathbb{R}^D$ for any non-uniform distribution $z \in p(z|z \in \mathbb{R}^{D>1}, \|z\| = 1)$ that is not singular.*

Proof. See Appendix E. \square

The proof is based on showing that Definition 1 holds also when expected similarity is higher than for uniformly distributed embeddings spaces as given by Lemma 1.

The shape of the non-uniform density $p(z)$ of common VLMs is a product of optimization by contrastive learning with random negative sampling [11]. Few general properties can be inferred for non-uniform densities. So et al. [85] finds that vision and text CLIP embeddings are distributed in separate modality-specific hyperspherical caps. Wang et al. [86] identifies the uniformity-alignment dilemma stating that perfect uniformity and alignment cannot be simultaneously achieved due to semantically similar but randomly sampled false negatives.

We found that using the probabilistic bound (12) for highly non-uniform VL embedding densities $p(z)$ results in poor estimates. The reason is that unrelated embeddings are far more similar than those for uniform distributions. Instead we propose a statistical sampling-based approach to obtain a probabilistic estimate for (9) in Definition 1 without requiring to estimate the non-uniform density $p(z)$. The probability in (12) is estimated by sampling N random semantic embeddings $z \sim p(z)$ and counting the number of samples being within the hyperspherical cone S_{cap}^{D-1} spanned by z^* and z_{min} (15) such that

$$P(\text{sim}(z^*, z) > \text{sim}(z^*, z')) \simeq \frac{1}{N} \sum_{i=1}^N \mathbf{1}_{S_{cap}^{D-1}}(z^{(i)}). \quad (16)$$

Our empirical results show that latent compositional semantic embeddings z^* are useful for all tested non-uniform VL embedding distributions. Additionally, the empirical estimate (16) provides an accurate measure of goodness.

D. Compositional discovery by gradient descent

The mathematical properties in Sec. III-B-III-C are derived while presuming all member semantics $z \in \mathcal{Z}$ are known. In this section we verify the possibility of finding latent compositional semantic embeddings z^* by iterative optimizing z^* one z at a time, instead of averaging the set \mathcal{Z} as in (10).

Proposition 2 (Discoverability III). *It is always possible to find an optimal compositional semantic embedding $z^* \in \mathbb{R}^D$ by iterative gradient descent optimization*

$$z^{*(t+1)} = z^{*(t)} - \lambda \nabla_{z^*} \left[\sum_{i=1}^L \text{sim}(z^{*(t)}, z^{(i)}) \right] \quad (17)$$

over random subsets $\tilde{\mathcal{Z}}^{(t)} \subseteq \mathcal{Z}$, $|\tilde{\mathcal{Z}}^{(t)}| = L$ given a sufficiently small learning rate λ .

Proof. See Appendix F. \square

The proof is based showing that the cosine similarity optimization objective is convex, and noting that all convex problems have global convergence guarantees.

IV. UNCONDITIONAL DENSE VISION-LANGUAGE MODEL

An unconditional dense VLM is a learned one-to-one function $f_\theta()$ that maps images $x \in \mathbb{R}^{3 \times H \times W}$ to dense embedding maps $Z \in \mathbb{R}^{D \times H \times W}$ consisting of aligned VL embeddings $z_{(i,j)} \in \mathbb{R}^D$ at point (i, j) in the image frame. The output Z represents observations abstracted into declarative semantic memories [35], [37], [38] which maximizes the predictive likelihood over past observations given x , without conditioning on an input text [13] or an image query [67]. Unconditional prediction [10], [11] is necessary for efficient open vocabulary spatio-semantic memory representations as explained in Sec. I. However, since objects have not one but several semantic descriptions [33]–[35], a single semantic embedding $z_{(i,j)}$ must simultaneously encode a multitude of task-relevant semantics.

We investigate the feasibility of discovering compositional semantics by f_θ as an image encoder-decoder dense prediction deep neural network architecture. To maximize the generality of our findings, f_θ is implemented by conceptually simple, general, and well-performing SOTA modules as shown in Fig. 3. A vision transformer (ViT) backbone [87] extracts visual features from image observations x . We use the ViT-Adapter [88] as a dense prediction task adapter to enhance the ViT backbone with vision-specific inductive biases. The adapter outputs a set of multi-scale feature maps $\mathcal{F} = \{F_1, F_2, F_3, F_4\}$. A Feature Pyramid Network (FPN) [89] integrates \mathcal{F} into a single feature map F . A simple decoder head bilinearly upsamples F into the input image resolution and do a final 1×1 convolution to project features into normalized semantic embedding maps Z .

In the remainder of this section, we explain how in fact dense latent compositional semantic embedding maps Z^* are discovered by an unconditional dense VLM f_θ when trained to predict Z .

A. Model training

The model f_θ is initialized with pretrained backbone parameters and trained end-to-end to predict semantic embedding maps Z from images x and dense annotations. Annotations consists of K types of paired semantic text descriptions $t^{(k)}$ encoded into semantic embeddings $z^{(k)}$, and boolean image masks $y \in \mathbb{B}^{H \times W}$ specifying which image elements $x_{(i,j)}$ are associated with t . We denote an observation n as a tuple $(x, t, y)_n$.

We use the contrastive learning objective

$$\mathcal{L}_{CL} = \mathbb{E} \left[-\log \frac{e^{\text{sim}(z, z^{(k)})/\tau}}{e^{\text{sim}(z, z^{(k)})/\tau} + \sum_{k'} e^{\text{sim}(z, z^{(k')})/\tau}} \right] \quad (18)$$

with temperature τ to optimize f_θ to predict z similar to $z^{(k)}$ for elements specified by y and negative samples $z^{(k')}$. The set of negative samples $\mathcal{Z}' = \mathcal{Z} \setminus \{z^{(k)}\}$ consists of all

known annotated semantics \mathcal{Z} in the dataset except the current sample annotation $z^{(k)}$. We optimize over all \mathcal{Z}' for every batch instead of randomly sampling negatives as the number of semantics are tractable. We note that the general objective (18) is equivalent to the previously proposed cross-entropy over softmax normalized embedding similarity objective [10]

$$\mathcal{L}_{CE} = \mathbb{E} \left[-(c^{(k)})^T \log \sigma \left(\text{sim}(\hat{z}, z^{(k)}) / \tau \right) \right] \quad (19)$$

with $c^{(k)}$ denoting one-hot class or description type vectors, $\sigma(\cdot)$ as the softmax function. The equivalence is apparent by zeroing out all but the one-hot true target embedding resulting from the dot product sum and expanding the softmax function

$$\mathcal{L}_{CE} = \mathbb{E} \left[0 - \dots - \log \frac{e^{\text{sim}(\hat{z}, z^{(k)}) / \tau}}{\sum_{k'=1}^K e^{\text{sim}(\hat{z}, z^{(k')}) / \tau}} - \dots - 0 \right]. \quad (20)$$

Next we verify that the objective (18), and equivalently (19), can learn latent compositional semantic embeddings z^* from independent nonoverlapping descriptions. Proposition 2 proves that z^* can be learned by gradient descent. We can therefore presume without loss of generality, that two descriptions $z^{(k_1)}$ and $z^{(k_2)}$ appear simultaneously in a batch for two independent but visually similar objects x_1 and x_2 mapping to the same latent semantic z . The combined loss is

$$\begin{aligned} \mathcal{L} &= \frac{1}{2} \left(\mathcal{L}_{CL}(z, z^{(k_1)}) + \mathcal{L}_{CL}(z, z^{(k_2)}) \right) \\ &= \frac{1}{2} \left(-\log \frac{1}{c} e^{\text{sim}(z, z^{(k_1)})} - \log \frac{1}{c} e^{\text{sim}(z, z^{(k_2)})} \right) \\ &= -\frac{1}{2} \left(\log e^{\text{sim}(z, z^{(k_1)})} + \log e^{\text{sim}(z, z^{(k_2)})} - 2 \log c \right) \\ &= -\frac{1}{2} \left(\text{sim}(z, z^{(k_1)}) + \text{sim}(z, z^{(k_2)}) \right) + \log c \end{aligned} \quad (21)$$

As the optimal z minimizing (21) equals the centroid of $z^{(k_1)}$ and $z^{(k_2)}$, the optimal z is the optimal latent compositional semantic embedding z^* as proved by Theorem 1. We conclude that the iterative optimization by objective (18) enable f_θ to learn z^* from visual similarity and nonoverlapping descriptions.

B. Sufficient similarity inference method

Conventional semantic segmentation presume an input image can be sensibly partitioned into a set of K fixed hand-crafted semantic classes \mathcal{E}_K . Each class k is represented by a one-hot embedding $e^{(k)} \in \mathcal{E}_K$. The embeddings \mathcal{E}_K span different dimensional axes on the positive quadrant of the unit hypersphere S^{K-1} . The partitioning is computed by assigning class k^* represented by the most similar embedding $e^{(k)}$ to each predicted embedding \hat{z}

$$k^* = \arg \max_k \left[\text{sim}(\hat{z}, e^{(k)}) \right] \quad \forall e^{(k)} \in \mathcal{E}_K. \quad (22)$$

Open world semantic segmentation likewise partition the image by assigning the most similar semantic k^* in a set of word semantics \mathcal{Z}_K distributed over S^{K-1} . The semantics of \mathcal{E}_K defines the orthogonal basis of S^{K-1} and thus limit queryable semantics to \mathcal{E}_K . In contrast, learning word semantics results

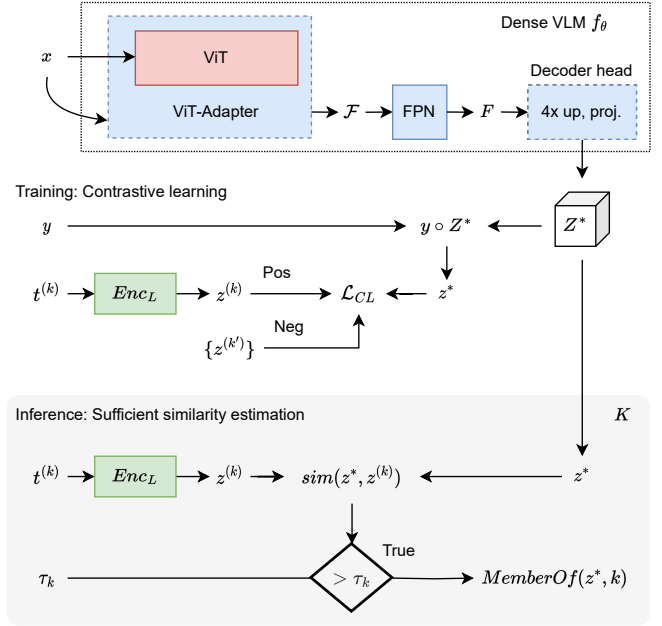


Fig. 3. The unconditional dense VLM f_θ transforms an image x into an embedding map Z^* representing compositional semantics z^* for every pixel. During training, predictions z^* for elements masked by y are optimized to be similar to targets $z^{(k)}$ and dissimilar to all other semantics $z^{(k')}$ generated from text descriptions $t^{(k)}$ by a language encoder Enc_L . During inference, z^* allows querying multiple semantics K by similarity. All elements above the similarity threshold τ_k are members of the semantic group k . τ_k is set to maximize likelihood of predicting past observations.

in a semantically meaningful orthogonal basis, allowing any \mathcal{Z}_K to be defined and queried at inference time.

Boyi et al. [10] identifies two weaknesses of the most similar partitioning approach: First, any object such as a *window-on-a-building-facade* can both be described as a “window” as well as part of a “building” at a higher-level. Hard partitioning by highest similarity haphazardly predicts one or the other. Secondly, hard partitioning assigns a semantic to every image element even if all queried semantics have low similarity with the image content. An example is a dog queried by the two semantics “grass” and “toy” is interpreted as “toy”. The use of abstract word semantics like “other” as a substitute for unspecified semantics is not a principled solution as there is no guarantee that the similarity between z^* and queried but unrelated semantic $z^{(k)}$ is less similar than the ambiguous semantic meaning of “other”

$$\text{sim}(z^*, z_{other}) \stackrel{?}{>} \text{sim}(z^*, z^{(k)}) \quad \forall z^{(k)} \in \mathcal{Z}_K. \quad (23)$$

We propose sufficient similarity as a principled inference method that allows semantic overlap and empty query results by a single compositional semantic embedding z^* . To evaluate semantic membership by sufficient similarity, we first compute a set of similarity threshold values $T = \{\tau_1, \dots, \tau_K\}$ for each known semantic $k \in \{1, \dots, K\}$. The value of τ_k is found by maximizing the likelihood that $\text{sim}(z^*, z^{(k)}) > \tau_k$ for true elements in past observations. At evaluation time, instead of selecting the most similar semantic k^* in (22), any similarity with semantic $z^{(k)}$ higher than the threshold τ_k are deemed sufficiently similar to be a member of the semantic group k

$$\text{sim}(z^*, z^{(k)}) > \tau_k \Rightarrow \text{MemberOf}(z^*, k). \quad (24)$$

We view (24) as a practical probabilistic approach for finding the mathematically derived hyperspherical cap S_{cap}^{D-1} (15) defining the membership set \mathcal{Z} (8) that maximizes the likelihood over past observations. For simplicity, we estimate a single maximum likelihood value τ_k for each semantic k by a logistic regression model. To fit the model, a set of similarity values $sim(z^*, z)$ are sampled from positive and negative elements of k using annotations y . The optimal τ_k is the the decision boundary or $sim(z^*, z)$ value that best separates positive and negative elements according to the model

$$p(\text{MemberOf}(sim(z^*, z), k)) = 0.5. \quad (25)$$

However, our method is not fundamentally limited to estimating only single constant values τ_k . To the best of our knowledge, the similarity thresholding method proposed by Cui et al. [90] is closest to our approach. While Cui et al. uses thresholding for uncertainty estimation, we propose thresholding to determine category membership (4).

V. EXPERIMENTS

In the following sections we set out to verify the properties and discoverability of latent compositional semantic embeddings derived in Sec. III and IV. We perform experiments on embedding spaces for three commonly used models: the VLMs CLIP [11] and OpenCLIP [12], and the language model SBERT [50]. Additionally, we do experiments on ideal uniformly distributed embedding spaces $U(S^{D-1})$ for comparison.

The first set of experiments investigates the lower bound capacity for compositional semantic embedding z^* to representing an arbitrary set of K sampled VL embeddings. The second experiment set analyzes the expected capacity for z^* to represent object descriptions with K semantic. The third experiment set verifies that z^* are be discoverable from visual appearance and nonoverlapping semantic annotations when training open-vocabulary unconditional dense VLMs.

Our experiments and results are relevant for any spatio-semantic representation method based on projecting image semantics to 3D or 2D coordinates [21], [32]. We believe evaluation in a general-purpose image dataset such as COCO-Stuff is a more valuable indicator than demonstrating our method on a comparatively narrow 3D dataset. The expected semantic prediction performance for image-frame and projected semantic point cloud inference is equivalent [32].

A. Experiment 1: z^* from random semantics

We estimate the lower bound capacity of z^* by sampling K embeddings z forming an object description set \mathcal{Z} of random semantics. Next we compute the optimal z^* by (10) and measure the separation between 100,000 randomly sampled embeddings Z' and the set \mathcal{Z} represented by z^* . Separability is measured by (16) approximating (12) for uniform and nonuniform distributions. High separability means it is highly unlikely any non-related random semantic is closer to z^* than the least close related semantic $z_{min} = \arg \min(Z)$. In other words, z^* has high cosine similarity (3) only with semantics z of the object description \mathcal{Z} .

To generate embeddings, we sample words from the English lexical database WordNet [91]. Sampled words gets transformed into a semantic embedding z by the models' language encoders. Ideally distributed embeddings are sampled uniformly on the hypersphere $U(S^{D-1})$. CLIP experiments use the largest available ViT-L/14@336px model generating 768 dimensional embeddings. For OpenCLIP we use the largest ViT-bigG-14 model, pretrained on the laion2b_s39b_b160k dataset, generating 1280 dimensional embeddings. SBERT uses the all-mpnet-base-v2 model generating 768 dimensional embeddings. We measure performance of object descriptions \mathcal{Z} of varying length K to estimate maximum representation capacity of z^* for each embedding space. Two additional experiments for higher dimensional embeddings explore the theoretical limits of z^* for large object descriptions \mathcal{Z} . Each experiment is repeated 1000 times for statistical estimation.

B. Experiment 2: z^* from object descriptions

The second set of experiments estimates the separability for 500 realistic object descriptions consisting of related semantics. Each object description is generated by a large language model (LLM)¹ and consists of K descriptive semantics including names, properties, and affordances. The results represent expected representational capacity of z^* in practical application.

C. Experiment 3: z^* from visual appearance

The third experiment set investigates if z^* can be discovered from independent observations of visual appearance paired with nonoverlapping semantic descriptions. To answer this question, we train dense VLM models f_θ introduced in Sec. IV on three variants of the COCO-Stuff dataset [92]. The first variant measures performance on the original 172 classes converted into semantic embeddings $z^{(k)}$. The second variant introduces compositional semantics by uniformly sampling a description from one of the three levels from the official label hierarchy (e.g. a *car-object* object described as "car", "vehicle", or "outdoor"). The third variant weights sampling so all descriptions are equally distributed over the dataset. Uniform and weighted sampling represent the long-tail distribution over low- and high-level semantics, respectively. Each image annotation is sampled only once, meaning compositional semantics must be learned by generalizing from independent observations of visual appearance. Additionally, we estimate separability (16) and similarity of the learned z^* embeddings with the optimal z_{opt}^* computed as the centroid of the ground truth word semantics (10). We evaluate results by IoU computed by the conventional most similar partitioning and our proposed sufficient similarity method introduced in Sec. IV-B. To use sufficient similarity we precompute τ_k for every semantic category k from 2000 samples from the training dataset covering all semantics.

We investigate how well existing methods represent compositional semantics by three representative baseline models. Our ZSSeg [14] implementation generates region proposals

¹Claude 2 provided by Anthropic (claude.ai)

by SAM [93] and uses CLIP [11] to predict semantic embeddings z . ConceptFusion [25] represent methods attempting to enhance CLIP-based methods. LSeg [10] is a popular unconditional dense VLM similar to our model. We initialize LSeg by the publicly available model weights optimized over seven datasets incl. COCO-Stuff. Our compositional semantic segmentation model (CSSeg) is optimized on COCO-Stuff for 160K iterations on four A6000 GPUs with a total batch size 4 and $0.75e-4$ learning rate. The ViT backbone is initialized with BEiT model weights [94]. We emphasize that our study concerns the practical feasibility of learning compositional semantics across a variety of models. We expect that more recent SOTA models [19], [88] are likely to further improve performance beyond our simple CSSeg model implementation.

VI. RESULTS

Here we present results demonstrating the capacity of latent compositions embeddings z^* for representing rich object descriptions in different embedding spaces. We also demonstrate that z^* can be learned by unconditional dense VLM from nonoverlapping annotations.

A. Experimental results 1: z^* from random semantics

Here we provide results and findings for z^* representing sets \mathcal{Z} of randomly sampled semantics z . Table I shows the expected similarity between z^* and object description semantics z is always higher than for unrelated semantics z' . The results verifies that z^* for all embedding distributions and object description sizes K satisfy Definition 1 for compositional embeddings. Table II shows lower bound separability of related $z \in \mathcal{Z}$ and non-related semantics $z' \in \mathcal{Z}'$ by z^* . All embedding spaces allow reliable separability for small object descriptions $K \leq 3$. For intermediate descriptions $K \leq 5$ separability of CLIP embeddings reduces to chance. SBERT maintains strong separability. Only ideal uniform distributions achieve perfect separability for large descriptions $K \leq 10$. Table III shows that sufficiently high-dimensional uniformly distributed embedding spaces can represent very large object descriptions of size $K \leq 100$ with perfect separability. Note that largest 4096 dimension embedding space equals the ResNet output embedding map dimension [95]. The probabilistic bound (12) accurately predict the empirical separation probability result for uniform distributions. The bound fails for highly non-uniform distributions as expected. Figure 4 visualizes embedding similarity distributions for different embedding spaces and object descriptions sizes K . Figure 5 shows how increasing dimensionality gradually improves separability.

The experiments verify the following mathematical results: Definition 1 for z^* , Theorem 1 about finding the optimal z^* , the separability bound of Theorem 2, and Proposition 1 concerning finding z^* for non-uniform distributions. We find that the object description size K representable by z^* is only constrained by embedding space dimensionality D and sufficient uniformity. The CLIP embedding space is less useful than OpenCLIP. The pure language model SBERT has better embedding space than both VLM models. We propose to

TABLE I
COMPOSITIONAL SEMANTICS EXPECTATION DELTA

$$\Delta \mathbb{E} = \mathbb{E} \text{sim}(z^*, z) - \mathbb{E} \text{sim}(z^*, z')$$

Distribution	$K = 3$	$K = 5$	$K = 10$
CLIP [11] ^a	0.119 (0.070)	0.083 (0.032)	0.043 (0.024)
OpenCLIP [12] ^b	0.245 (0.032)	0.156 (0.027)	0.083 (0.020)
SBERT [50] ^a	0.397 (0.040)	0.273 (0.035)	0.156 (0.026)
$U(z)_{D=768}$	0.577 (0.012)	0.447 (0.010)	0.316 (0.080)
$U(z)_{D=1280}$	0.577 (0.010)	0.447 (0.080)	0.316 (0.006)
$U(z)_{D=2048}$	0.577 (0.008)	0.447 (0.006)	0.316 (0.005)
$U(z)_{D=4096}$	0.577 (0.005)	0.447 (0.005)	0.316 (0.003)

a: $D = 768$, b: $D = 1280$

TABLE II
SEPARATION OF RELATED AND NONRELATED RANDOM SEMANTICS

$$P(\text{sim}(z^*, z) > \text{sim}(z^*, z'))$$

Distribution	$K = 3$	$K = 5$	$K = 10$
CLIP [11] ^a	0.954 (0.117)	0.533 (0.261)	0.187 (0.143)
OpenCLIP [12] ^b	1.000 (0.001)	0.907 (0.115)	0.400 (0.180)
SBERT [50] ^a	1.000 (0.002)	0.977 (0.043)	0.647 (0.188)
$U(z)_{D=768}$	1 (0)	1 (0)	1 (0)
$U(z)_{D=1280}$	1 (0)	1 (0)	1 (0)
$U(z)_{D=2048}$	1 (0)	1 (0)	1 (0)
$U(z)_{D=4096}$	1 (0)	1 (0)	1 (0)

a: $D = 768$, b: $D = 1280$

TABLE III
LARGE OBJECT DESCRIPTION EXPECTATION DELTA AND SEPARATION

$$K = 100$$

Distribution	$\Delta \mathbb{E}$	$P(\text{sim}(z^*, z) > \text{sim}(z^*, z'))$	
		Empirical (16)	Bound (12)
CLIP [11] ^a	0.004 (0.008)	0.011 (0.011)	1.0*
OpenCLIP [12] ^b	0.009 (0.007)	0.013 (0.012)	1.0*
SBERT [50] ^a	0.018 (0.009)	0.015 (0.013)	1.0*
$U(z)_{D=768}$	0.010 (0.001)	0.605 (0.148)	0.612
$U(z)_{D=1280}$	0.010 (0.002)	0.838 (0.116)	0.863
$U(z)_{D=2048}$	0.010 (0.002)	0.967 (0.040)	0.988
$U(z)_{D=4096}$	0.010 (0.001)	1.000 (0.001)	1.000

a: $D = 768$, b: $D = 1280$, *: Erroneous due to strong non-uniformity

TABLE IV
SEPARATION FOR REALISTIC OBJECT DESCRIPTIONS

$$P(\text{sim}(z^*, z) > \text{sim}(z^*, z'))$$

Distribution	$K = 3$	$K = 5$	$K = 10$
CLIP [11] ^a	1.000 (0.001)	0.976 (0.059)	0.745 (0.192)
OpenCLIP [12] ^b	1 (0)	0.996 (0.015)	0.877 (0.146)
SBERT [50] ^a	1 (0)	1.000 (0.001)	0.981 (0.056)

a: $D = 768$, b: $D = 1280$

learn unconditional dense VLMs on language model embeddings instead of global description VLMs like CLIP as the pretrained vision encoder is not used. The findings motivate further work towards increasing uniformity of existing VLM embedding distributions to better leverage the capacity of high-dimensional embedding spaces and to improve discriminability of semantic embeddings [85], [96].

B. Experimental results 2: z^* from object descriptions

Here we provide separability results for z^* representing sets \mathcal{Z} of realistic object descriptions composed of related semantics z . Table IV shows that sets of related semantics have better separability than the lower bound of random semantic descriptions presented in Table II. Both CLIP and OpenCLIP achieve strong separability for $K \leq 5$, and SBERT allows large object representations of $K \leq 10$.

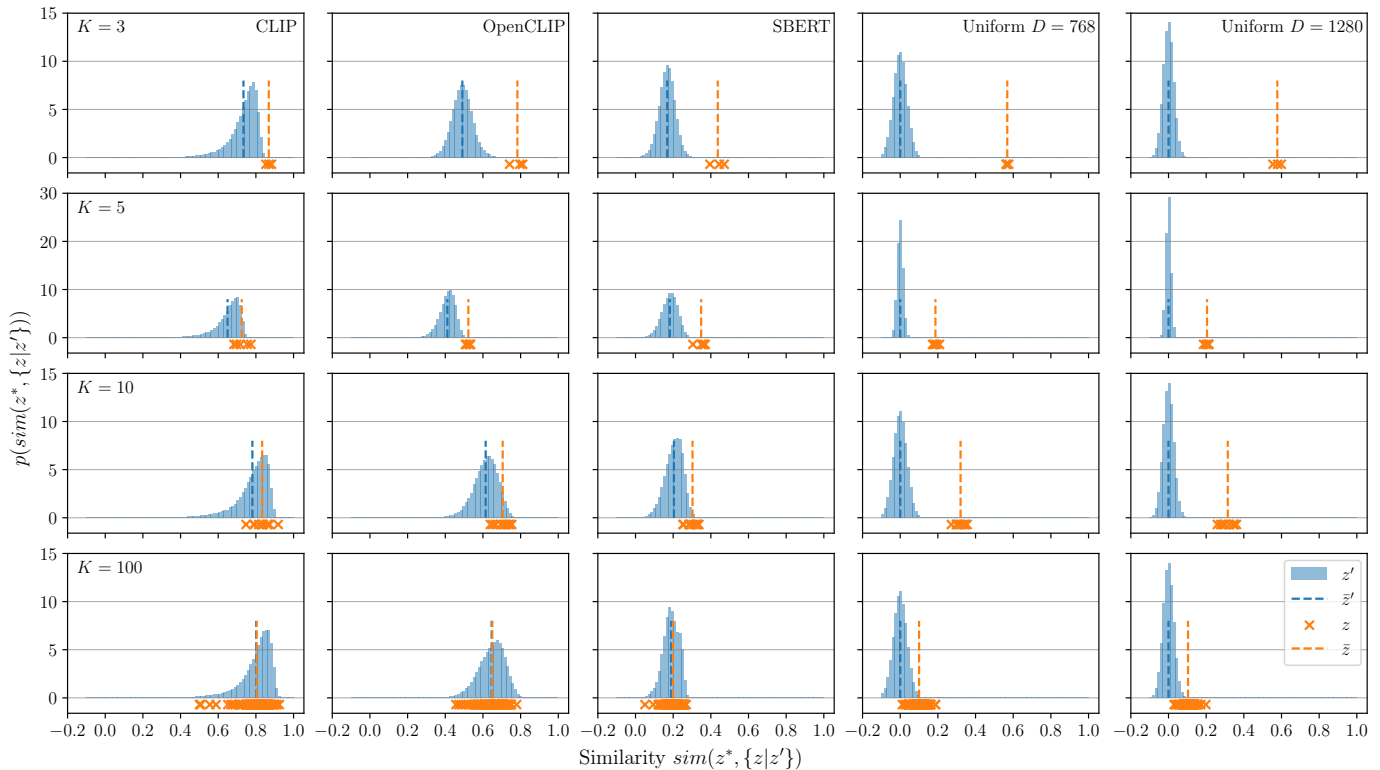


Fig. 4. Similarity distributions between a latent compositional semantic embedding z^* and all object description embeddings $z \in \mathcal{Z}$ it represent (orange) and randomly sampled unrelated word embeddings z' (blue). Columns show different embedding spaces. Each row shows object descriptions of different size K . A z^* is useful if it separates the distribution of z and z' by cosine similarity (3).

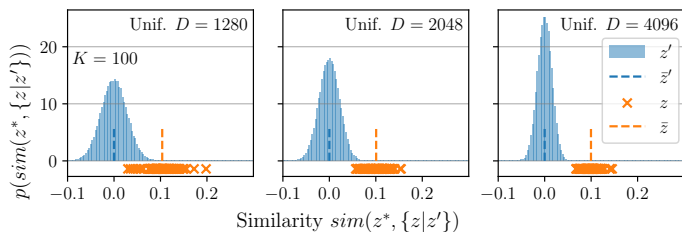


Fig. 5. Similarity distributions for large object descriptions \mathcal{Z} in very high-dimensional uniformly distributed embedding spaces.

Figure 6 visualizes similarity distributions for three realistic object descriptions. The top row shows distributions for the short object description of a “medium-sized utility vehicle” $\mathcal{Z}_1 = \{\text{truck, van, vehicle}\}$. All z are perfectly separable from the distribution of z' by z^* . The middle row shows the separability of a medium sized description for a “patch on a drivable flat asphalt road with painted lane markings” $\mathcal{Z}_2 = \{\text{road, lane marking, drivable, asphalt, flat}\}$. CLIP, OpenCLIP, and SBERT allow reliable separation with 99.1 %, 99.6 %, and 100 % confidence. The bottom row visualizes the distribution of a large description of a “white wooden table surface” $\mathcal{Z}_3 = \{\text{'table', 'wood', 'counter', 'solid', 'surface', 'white', 'static', 'flat', 'furniture', 'static'}\}$. The CLIP embedding space struggles by reaching only 75 % confidence. The OpenCLIP and SBERT distributions performs better with 86 % and 99 % confidence.

We conclude that SBERT embedding are practically useful even for large realistic object descriptions up to about 10 semantics.

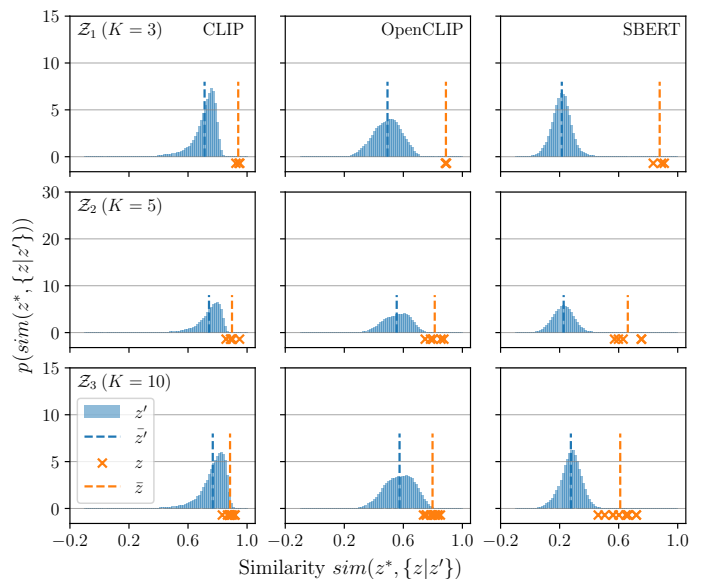


Fig. 6. Similarity distributions for three realistic object descriptions \mathcal{Z}_i of varying sizes K (orange) and randomly sampled word embeddings z' (blue).

C. Experimental results 3: z^* from visual appearance

Here we present results showing it is possible to discover compositional semantics z^* from independent observations of visual appearance paired and single object descriptions. We provide results for models trained on CLIP or SBERT semantic embeddings z . In Table V we show segmentation performance on the original COCO-Stuff class labels as VL embeddings. Our CSSeg model results are labeled by *. A large performance discrepancy exist between region proposal and global VLM models and learned VLMs. We conclude

TABLE V
OPEN VOCABULARY SEGMENTATION ON COCO-STUFF

	mIoU	mAcc
ZSSeg [14]	10.77	28.71
ConceptFusion [25]	10.77	29.00
LSeg [10]	37.37	52.20
CSSeg (CLIP)*	47.10	60.61
CSSeg (SBERT)*	48.21	61.90

TABLE VI
COMPOSITIONAL SEMANTICS ON COCO-STUFF
mIoU

		All levels	Level 1	Level 2+3	
ZSSeg	SS	5.75	5.60	6.73	
	MS	10.64	11.18	2.88	
ConceptFusion	SS	5.66	5.50	6.67	
	MS	10.66	11.19	2.89	
LSeg	SS	26.82	27.99	16.12	
	MS	37.12	39.27	13.98	
CSSeg (CLIP)*	US	SS	32.99	31.94	55.93
		MS	25.90	26.10	33.27
	WS	SS	37.89	37.67	48.82
		MS	45.94	48.63	12.18
CSSeg (BERT)*	US	SS	38.19	37.15	57.38
		MS	24.95	24.84	32.39
	WS	SS	42.23	40.85	55.57
		MS	45.67	48.33	12.26

US: Uniform sampling, WS: Weighted sampling
SS: Sufficient similarity evaluation, MS: Most similar evaluation

that strong dense embedding prediction performance benefit from a dedicated semantic segmentation model in diverse and complex scenes represented by COCO.

Table VI shows evaluation results for compositional semantics. Each model is evaluated by our proposed sufficient similarity (SS) and the conventional most similar (MS) method. We present results for two dataset variants; uniform sampling (US) and weighted sampling (WS) as described in Sec. V-C. Levels specify which hierarchical semantic levels are being queried (e.g. level 1 *cat*, level 2 *animal*, and level 3 *outdoor*). The strong higher-level semantics performance prove that compositional semantics can be learned from visual observation and accurately queried by sufficient similarity. The performance difference between US and WS shows that higher-level semantics can be learned from relatively few examples compared with low-level semantics. The CSSeg model trained on overlapping semantics outperform the best model trained on original semantics when evaluated by the conventional MS method. This result indicate the potential of our approach to allow querying overlapping semantics while still outperforming conventional non-overlapping semantics models with a more sophisticated sufficient similarity threshold estimation method. See Figure 1 and 7 for visualizations.

Figure 8 visualizes the mean similarity distribution between learned z^* and optimal z_{opt}^* embeddings. Learned z^* embeddings have a similarity or alignment gap with the original VL embedding spaces [86], [97]. However, the strong results in Table VI proves that learned z^* have adequate relative similarity with z_{opt}^* for sufficient similarity segmentation in practice, at least for small semantic sets \mathcal{Z} . For larger \mathcal{Z} , the low alignment will likely reduce performance due to unintended similarity with unrelated semantics [97].

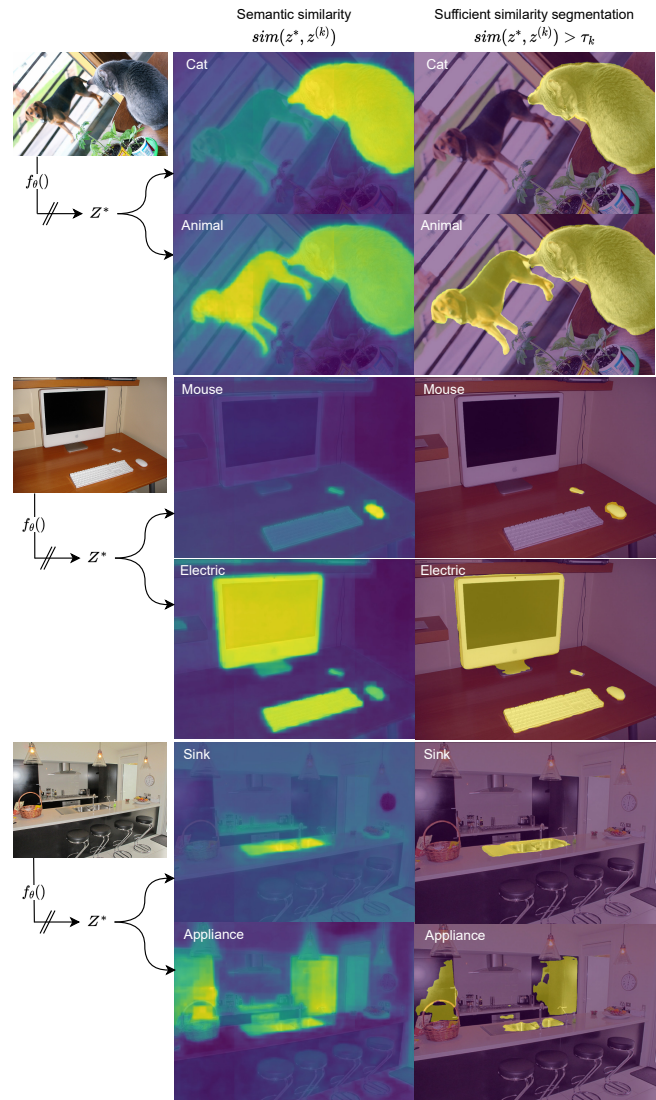


Fig. 7. Examples of overlapping semantics inferable from latent compositional semantic embeddings z^* representing learned object descriptions \mathcal{Z} . The 3rd and 4th examples illustrate failure cases related to sufficient similarity threshold τ_k estimation for low- and high-level semantics, respectively.

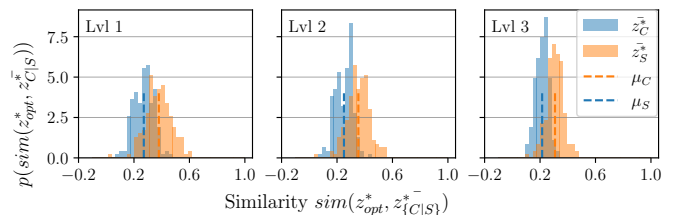


Fig. 8. The distribution of mean similarities between optimal z_{opt}^* and learned z^* CLIP (blue) and SBERT (orange) embeddings for three semantic levels.

VII. CONCLUSIONS

In this paper, we present a mathematical analysis and experimental verification of latent compositional semantic embeddings z^* as a learnable knowledge representation for rich object descriptions satisfying the requirements of spatio-semantic representations. Our VLM method is limited by the similarity gap between predicted z^* and optimal z_{opt}^* . For future work, we propose a dynamic approach to infer sufficient similarity thresholds τ_k which takes into account environment

and task context. Additionally, we propose a learning objective optimizing for absolute similarity or greater alignment in addition to relative similarity (18). We hope our findings will contribute towards greater understanding of what semantics unconditional dense VLMs learn, and the theoretical limit of semantic expressivity of learned representations. Additionally, we hope to encourage more work towards learning and inferring compositional and overlapping semantics, and provide motivation for improving uniformity of VL embedding spaces.

ACKNOWLEDGMENTS

This work was financially supported by JST SPRING, Grant Number JPMJSP2125. The authors would like to take this opportunity to thank the ‘‘Interdisciplinary Frontier Next-Generation Researcher Program of the Tokai Higher Education and Research System’’.

The authors would like to thank Minh-Quan Dao, Yingjie Niu, Keisuke Fujii, and Kento Ohtani for proofreading and constructive criticism of the manuscript.

APPENDIX MATHEMATICAL PROOFS

Here we provide full mathematical proofs for all theorems, propositions, and lemmas.

A. Proof for Lemma 1

Proof. All normalized semantic embeddings z are vectors in the set of vectors constituting the unit hypersphere

$$z \in S^{D-1} = \{z \in \mathbb{R}^D : \|z\| = 1\}. \quad (26)$$

The distribution of uniformly sampled random vectors $Z \sim U(S^{D-1})$ is isotropic (i.e. properties rotationally invariant). The covariance matrix Σ of isotropic distributions equals the diagonal matrix I_D :

$$\Sigma(Z) = \mathbb{E} Z Z^T = I_D. \quad (27)$$

For the expected inner product of two independent random vectors $Z^{(i)}, Z^{(j)}$ sampled from an isotropic distribution it follows

$$\mathbb{E} \langle Z^{(i)}, Z^{(j)} \rangle^2 = \mathbb{E}_{Z^{(j)}} \mathbb{E}_{Z^{(i)}} \left[\langle Z^{(i)}, Z^{(j)} \rangle^2 | Z^{(j)} \right] \quad (28)$$

Assuming a particular but arbitrary vector $z^{(j)}$ and substituting (27) the inner expectation becomes

$$\begin{aligned} \mathbb{E}_{Z^{(i)}} \langle Z^{(i)}, z^{(j)} \rangle^2 &= z^{(j)T} \mathbb{E} \left[Z^{(i)} Z^{(i)T} \right] z^{(j)} \\ &= z^{(j)T} I_D z^{(j)} \\ &= z^{(j)T} z^{(j)} \\ &= \|z^{(j)}\|^2 \end{aligned} \quad (29)$$

The outer expectation after substituting (29) and (27) becomes

$$\begin{aligned} \mathbb{E}_{Z^{(i)}} \langle Z^{(i)}, z^{(j)} \rangle^2 &= \mathbb{E}_{Z^{(j)}} \|z^{(j)}\|^2 = \mathbb{E} Z^{(j)T} Z^{(j)} \\ &= \mathbb{E} \text{tr} \left[Z^{(j)T} Z^{(j)} \right] \\ &= \mathbb{E} \text{tr} \left[Z^{(j)} Z^{(j)T} \right] \\ &= \text{tr} \left[\mathbb{E} Z^{(j)} Z^{(j)T} \right] \\ &= \text{tr} [I_D] = D. \end{aligned} \quad (30)$$

Expanding the inner product of two normalized random Euclidean vectors $\hat{Z}^{(i)}, \hat{Z}^{(j)}$ sampled from an isotropic distribution

$$\begin{aligned} \mathbb{E} \langle \hat{Z}^{(i)}, \hat{Z}^{(j)} \rangle &= \mathbb{E} \hat{Z}^{(i)} \cdot \hat{Z}^{(j)} \\ &= \mathbb{E} \frac{Z^{(i)}}{\|Z^{(i)}\|} \cdot \frac{Z^{(j)}}{\|Z^{(j)}\|} \\ &= \mathbb{E} \frac{1}{\|Z^{(i)}\| \|Z^{(j)}\|} \langle Z^{(i)}, Z^{(j)} \rangle \\ &= \frac{\sqrt{D}}{\sqrt{D}\sqrt{D}} = \frac{1}{\sqrt{D}}. \end{aligned} \quad (31)$$

Taking the limit shows that any two random vectors are orthogonal in high-dimensional isotropic vector spaces

$$\lim_{D \rightarrow \infty} \mathbb{E} \langle \hat{Z}^{(i)}, \hat{Z}^{(j)} \rangle = 0. \quad (32)$$

As orthogonality is invariant to vector length

$$\mathbb{E} \langle \hat{Z}^{(i)}, \hat{Z}^{(j)} \rangle = \mathbb{E} \langle Z^{(i)}, Z^{(j)} \rangle = \frac{1}{\sqrt{D}}. \quad (33)$$

Noting that inner product $\langle Z^{(i)}, Z^{(j)} \rangle$ equals cosine distance similarity $\text{sim}(Z^{(i)}, Z^{(j)})$ for Euclidean spaces completes the proof. \square

B. Proof for Lemma 2

Proof. Supposing the optimal compositional semantic embedding z^* is found given a set of K sub-semantic embeddings $\mathcal{Z} = \{z^{(1)}, \dots, z^{(K)}\}$ such that

$$z^* = \arg \max \frac{1}{K} \sum_{i=1}^K \text{sim}(z^*, z^{(k)}) - \mathbb{E} \text{sim}(z^*, z') \quad (34)$$

where z' is a semantic embedding of any unrelated object description.

Note that the sub-semantics \mathcal{Z} can be ordered by similarity with z^* , and that the least similar sub-semantic z_{min} and its similarity value ϵ is known

$$z_{min} = \arg \min \text{sim}(z^*, z) \forall z \in \mathcal{Z}. \quad (35)$$

$$\epsilon = \text{sim}(z^*, z_{min}). \quad (36)$$

A hyperspherical cap S_{cap}^{D-1} is defined by z^* as the normal center vector and the angle θ_{min} between z^* and z_{min}

$$S_{cap}^{D-1} = \{z \in \mathbb{R}^D : \|z\| = 1, \theta_z \leq \theta_{min}\} \quad (37)$$

where the angles θ are related to similarities by

$$\theta_z = \arccos(\text{sim}(z^*, z)) \quad (38)$$

$$\theta_{min} = \arccos(\text{sim}(z^*, z_{min})). \quad (39)$$

Since

$$\text{sim}(z^*, z) \geq \text{sim}(z^*, z_{min}) \Leftrightarrow \theta_z \leq \theta_{min} \quad \forall z \in \mathcal{Z} \quad (40)$$

$$\text{sim}(z^*, z^*) = 1 \Leftrightarrow \theta_{z^*} = 0 < \theta_{min} \quad (41)$$

all $z \in \mathcal{Z}$ and z^* are in S_{cap}^{D-1} . \square

C. Proof for Theorem 1

Proof. The optimal compositional semantic embedding $z^* \in \mathbb{R}^D$ representing a set of K sub-semantics $z \in \mathcal{Z}$ in a uniform distribution over the unit hypersphere $U(S^{D-1})$ is

$$z^* = \arg \max \sum_{i=1}^K \text{sim}(z^*, z^{(i)}) = \arg \max \sum_{i=1}^K (z^*)^T z^{(i)}. \quad (42)$$

Maximizing cosine distance similarity $\text{sim}(z^*, z)$ is equivalent to minimizing squared distance $\|z^* - z\|^2$ on the unit hypersphere as

$$\begin{aligned} \min \sum_{i=1}^K \|z^* - z^{(i)}\|^2 &= \sum_{i=1}^K (z^* - z^{(i)})^T (z^* - z^{(i)}) \\ &= \min \sum_{i=1}^K \left[\|z^*\|^2 - 2(z^*)^T z^{(i)} + \|z^{(i)}\|^2 \right] \\ &= \min \sum_{i=1}^K \left[2 - 2(z^*)^T z^{(i)} \right] \\ &= \min \left[2K - 2 \sum_{i=1}^K (z^*)^T z^{(i)} \right] \\ &\propto \min \left[- \sum_{i=1}^K (z^*)^T z^{(i)} \right] \\ &= \max \sum_{i=1}^K (z^*)^T z^{(i)} \end{aligned} \quad (43)$$

The vector z^* maximizing (42) can thus be found from the derivative with respect to the vector z^*

$$\frac{d}{dz^*} \sum_{i=1}^K \|z^* - z^{(i)}\|^2 = 0. \quad (44)$$

To apply the general chain rule [98], we rewrite (44) with variable substitution so that each operation in the function is factored into single variable components for easily finding partial differentials:

$$\begin{aligned} \sum_{i=1}^K \|z^* - z^{(i)}\|^2 &= g = \sum_{i=1}^K \|f\|^2 \\ f &= z^* - z^{(i)}. \end{aligned} \quad (45)$$

Applying the chain rule and noting that $\|f\|^2 = f^T f$ gives

$$\begin{aligned} \frac{\partial g}{\partial z^*} &= \frac{\partial g}{\partial f} \frac{\partial f}{\partial z^*} \\ &= \sum_{i=1}^K 2f^T \frac{\partial}{\partial z^*} (z^* - z^{(i)}) \\ &= 2 \sum_{i=1}^K (z^* - z^{(i)})^T \left[\frac{\partial}{\partial z_1^*} (z^* - z^{(i)}), \dots, \frac{\partial}{\partial z_D^*} (z^* - z^{(i)}) \right]^T \\ &= 2 \sum_{i=1}^K (z^* - z^{(i)})^T [e_1, \dots, e_D] \\ &= 2 \left[\sum_{i=1}^K (z_1^* - z_1^{(i)}), \dots, \sum_{i=1}^K (z_D^* - z_D^{(i)}) \right]^T = 0 \end{aligned} \quad (46)$$

where e_d is the one-hot vector with the d^{th} element set to 1. Equation (46) is an element-wise system of equations stating that for every d^{th} element

$$\sum_{i=1}^K (z_d^* - z_d^{(i)}) = 0 \quad (47)$$

meaning the optimal z^* maximizing (42) equals the centroid of the sub-semantics $z^{(i)} \in \mathcal{Z}$

$$z^* = \frac{1}{K} \sum_{i=1}^K z^{(i)}. \quad (48)$$

To prove z^* specified by (48) satisfies Definition 1 we write

$$\mathbb{E} \text{sim}(z^*, z) = \mathbb{E} \left[\left(\frac{1}{K} \sum_{i=1}^K z^{(i)} \right) \cdot z \right] = \frac{1}{K} \sum_{i=1}^K \mathbb{E} z^{(i)} \cdot z. \quad (49)$$

As z equals one of the $z^{(i)} \in \mathcal{Z}$ we can assume $z = z^{(k)}$ without loss of generality and expand the sum in (49) as

$$\begin{aligned} \mathbb{E} \text{sim}(z^*, z) &= \frac{1}{K} \left(\mathbb{E}[z^{(1)} \cdot z^{(k)}] + \dots \right. \\ &\quad \left. + \mathbb{E}[z^{(k)} \cdot z^{(k)}] + \dots + \mathbb{E}[z^{(K)} \cdot z^{(k)}] \right) \end{aligned} \quad (50)$$

We find a lower bound for (50) by applying Lemma 1 and noting that the expected similarities $\text{sim}(z^{(i)}, z^{(j)}) \forall z^{(i)}, z^{(j)} \in \mathcal{Z}$ must be higher or equal to random vectors, and that $z^{(k)} \cdot z^{(k)} = 1$

$$\begin{aligned} \mathbb{E} \text{sim}(z^*, z) &\geq \frac{1}{K} \left(D^{-\frac{1}{2}} + \dots + 1 + \dots + D^{-\frac{1}{2}} \right) \\ &= \frac{1}{K} \left((K-1)D^{-\frac{1}{2}} + 1 \right). \end{aligned} \quad (51)$$

Substituting the bound (51) into Definition 1 and applying Lemma 1 on the RHS

$$\mathbb{E} \text{sim}(z^*, z) \geq \frac{1}{K} \left((K-1)D^{-\frac{1}{2}} + 1 \right) > D^{-\frac{1}{2}}. \quad (52)$$

Rearranging the two leftmost inequalities in (52)

$$(K-1)D^{-\frac{1}{2}} + 1 > KD^{-\frac{1}{2}} \quad (53)$$

$$KD^{-\frac{1}{2}} - D^{-\frac{1}{2}} + 1 - KD^{-\frac{1}{2}} > 0 \quad (54)$$

$$-D^{-\frac{1}{2}} > -1 \quad (55)$$

$$D^{-\frac{1}{2}} < 1 \quad (56)$$

$$\sqrt{D} > 1 \quad (57)$$

which is true for $D > 1$ and thus proves Theorem 1. \square

D. Proof for Theorem 2

Proof. A random vector z' sampled from the uniform distribution over the unit hypersphere $U(S^{D-1})$ is equally likely to be a point anywhere on S^{D-1} . The probability z' is sampled in a particular surface region $A_{D,r}$ is

$$P(z' \in A_{D,r}) = \frac{A_{D,r}}{A_D} \quad (58)$$

where A_D is the total surface region.

The probability z' is sampled into the surface region defined by the hyperspherical cap S_{cap}^{D-1} with surface area A_{cap} given in Lemma 2 is therefore

$$P(z' \in S_{cap}^{D-1}) = \frac{A_{cap}}{A_D}. \quad (59)$$

The surface area ratio of a hyperspherical cap [96] is

$$A_{D,r} = \frac{1}{2} A_D I_{\sin^2(\theta)}\left(\frac{D-1}{2}, \frac{1}{2}\right) \quad (60)$$

where $I_x(a, b)$ is the regularized incomplete beta function.

Substituting (60) into (58) gives

$$P(z' \in S_{cap}^{D-1}) = \frac{1}{2} I_{\sin^2(\theta)}\left(\frac{D-1}{2}, \frac{1}{2}\right). \quad (61)$$

The probability that z' is not sampled in S_{cap}^{D-1} is

$$\begin{aligned} P(z' \notin S_{cap}^{D-1}) &= 1 - P(z' \in S_{cap}^{D-1}) \\ &= 1 - \frac{1}{2} I_{\sin^2(\theta)}\left(\frac{D-1}{2}, \frac{1}{2}\right). \end{aligned} \quad (62)$$

By Lemma 2 and (39) we know

$$\forall z' \quad \text{sim}(z^*, z_{min}) \geq \text{sim}(z^*, z') \Leftrightarrow z' \notin S_{cap}^{D-1}. \quad (63)$$

Substituting the bound $\text{sim}(z^*, z_{min})$ by (40) gives

$$\forall z', z \in \mathcal{Z} \quad \text{sim}(z^*, z) \geq \text{sim}(z^*, z') \Leftrightarrow z' \notin S_{cap}^{D-1}. \quad (64)$$

Substituting the LHS of (64) into (62) and recollecting (39) proves Theorem 2. \square

E. Proof for Proposition 1

Proof. Non-uniformity means the distribution of vectors is not maximally dispersed over the hypersphere [97]. Recalling Lemma 1 for uniform distributions, the expected similarity of two non-uniformly distributed independent vectors $Z^{(i)}, Z^{(j)} \sim p(Z)$ is therefore

$$\mathbb{E} \text{sim}(Z^{(i)}, Z^{(j)}) = C \geq \frac{1}{\sqrt{D}}. \quad (65)$$

By substituting (65) in Definition 1 gives

$$\mathbb{E} \text{sim}(z^*, z) > \mathbb{E} \text{sim}(z^*, z') = C. \quad (66)$$

Expanding the LHS of (66) using the same idea as in (49) and (50)

$$\mathbb{E} \text{sim}(z^*, z) \geq \frac{1}{K} [(K-1)C + 1]. \quad (67)$$

Substituting (67) into (66)

$$\frac{1}{K} [(K-1)C + 1] > C \quad (68)$$

$$KC - C + 1 > KC \quad (69)$$

$$-C > -1 \quad (70)$$

$$C < 1. \quad (71)$$

Since $\text{sim}(z^{(i)}, z^{(j)}) \in [-1, 1[$ s.t. $z^{(i)} \neq z^{(j)}$ the inequality (66) is true for all distributions $p(z)$ except the singular distribution and thus proves Proposition 1. \square

F. Proof for Proposition 2

Proof. The global convergence guarantee for convex optimization problems [99] proves that for any convex function f is guaranteed that the value $z^{*(t)}$ converges to the optimal value z^*

$$\lim_{t \rightarrow \infty} f(z^{*(t)}) = f(z^*) \quad (72)$$

given a sufficiently small learning rate λ .

We prove that the cosine similarity optimization objective (42) is a convex problem by noting that the set (26) is convex and show that the Hessian matrix

$$H(f(z^*)) = \nabla_{z^*}^2 f(z^*) = \left[\frac{\partial}{\partial z_i^* \partial z_j^*} f(z^*) \right] \quad (73)$$

is a positive semidefinite matrix [98]. Note that $f(z^*)$ substitutes $\sum_{k=1}^K \text{sim}(z^*, z^{(k)})$. Recalling the form of the first partial derivatives (46) and taking another partial derivative for an arbitrary element

$$\frac{\partial}{\partial z_i^* \partial z_j^*} f(z^*) = \frac{\partial}{\partial z_i^*} \left[K z_j^* - \sum_{k=1}^K z_j^{(k)} \right] = K \mathbf{1}_{i=j}. \quad (74)$$

The Hessian matrix is thus the scaled identity matrix

$$H(f(z^*)) = [K e_i] = K I_D \quad (75)$$

meaning $f(z^*)$ is a convex function.

Finally noting that

$$\mathbb{E} \left[\frac{1}{L} \sum_{i=1}^L z \in \mathcal{Z}^{(t)} \right] = \frac{1}{K} \sum_{i=1}^K z^{(i)} \in \mathcal{Z}, \quad \mathcal{Z}^{(t)} \subseteq \mathcal{Z} \quad (76)$$

shows that the optimal convergence value obtained by optimizing (42) by gradient descent results in the optimal compositional semantic embedding z^* obtained by (48). \square

REFERENCES

- [1] M. Ahn, A. Brohan, N. Brown *et al.*, “Do as i can and not as i say: Grounding language in robotic affordances,” in *arXiv preprint arXiv:2204.01691*, 2022.
- [2] D. Shah, B. Osinski, B. Ichter, and S. Levine, “LM-nav: Robotic navigation with large pre-trained models of language, vision, and action,” in *6th Annual Conference on Robot Learning (CoRL)*, 2022.
- [3] W. Huang, P. Abbeel, D. Pathak *et al.*, “Language models as zero-shot planners: Extracting actionable knowledge for embodied agents,” *arXiv preprint arXiv:2201.07207*, 2022.
- [4] A. Zeng, M. Attarian, B. Ichter *et al.*, “Socratic models: Composing zero-shot multimodal reasoning with language,” in *International Conference on Learning Representations (ICLR)*, 2023.

- [5] W. Huang, F. Xia, T. Xiao *et al.*, “Inner monologue: Embodied reasoning through planning with language models,” in *Proceedings of The 6th Conference on Robot Learning (CoRL)*, 2023, pp. 1769–1782.
- [6] J. Liang, W. Huang, F. Xia *et al.*, “Code as policies: Language model programs for embodied control,” in *preprint arXiv:2209.07753*, 2022.
- [7] K. Nottingham, P. Ammanabrolu, A. Suhr, Y. Choi, H. Hajishirzi, S. Singh, and R. Fox, “Do embodied agents dream of pixelated sheep?: Embodied decision making using language guided world modelling,” in *Workshop on Reincarnating Reinforcement Learning at ICLR*, 2023.
- [8] I. Singh, V. Blukis, A. Mousavian *et al.*, “Progprompt: Generating situated robot task plans using large language models,” in *Int. Conf. on Robotics and Automation (ICRA)*, 2023, pp. 11 523–11 530.
- [9] A. Brohan, N. Brown, J. Carbajal *et al.*, “Rt-2: Vision-language-action models transfer web knowledge to robotic control,” in *arXiv preprint arXiv:2307.15818*, 2023.
- [10] B. Li, K. Q. Weinberger, S. Belongie, V. Koltun, and R. Ranftl, “Language-driven semantic segmentation,” in *International Conference on Learning Representations (ICLR)*, 2022.
- [11] A. Radford, J. W. Kim, C. Hallacy *et al.*, “Learning transferable visual models from natural language supervision,” in *International Conference on Machine Learning (ICML)*, 2021, pp. 8748–8763.
- [12] C. Schuhmann, R. Beaumont, R. Vencu *et al.*, “LAION-5b: An open large-scale dataset for training next generation image-text models,” in *Thirty-sixth Conference on Neural Information Processing Systems Datasets and Benchmarks Track*, 2022.
- [13] G. Ghiasi, X. Gu, Y. Cui, and T.-Y. Lin, “Scaling open-vocabulary image segmentation with image-level labels,” in *Proceedings of the IEEE/CVF European Conference on Computer Vision (ECCV)*, 2022.
- [14] M. Xu, Z. Zhang, F. Wei, Y. Lin, Y. Cao, H. Hu, and X. Bai, “A simple baseline for open vocabulary semantic segmentation with pre-trained vision-language model,” *Proceedings of the IEEE/CVF European Conference on Computer Vision (ECCV)*, 2022.
- [15] Y. Rao, W. Zhao, G. Chen, Y. Tang, Z. Zhu, G. Huang, J. Zhou, and J. Lu, “Denseclip: Language-guided dense prediction with context-aware prompting,” in *Proceedings of the IEEE Conference on Computer Vision and Pattern Recognition (CVPR)*, 2022.
- [16] C. Zhou, C. C. Loy, and B. Dai, “Extract free dense labels from clip,” in *European Conference on Computer Vision (ECCV)*, 2022.
- [17] Z. T. Zheng Ding, Jieke Wang, “Open-vocabulary universal image segmentation with maskclip,” in *International Conference on Machine Learning (ICLR)*, 2023.
- [18] M. Xu, Z. Zhang, F. Wei, H. Hu, and X. Bai, “Side adapter network for open-vocabulary semantic segmentation,” in *2021 IEEE/CVF Conference on Computer Vision and Pattern Recognition (CVPR)*, 2023.
- [19] X. Zou, Z.-Y. Dou, J. Yang *et al.*, “Generalized decoding for pixel, image, and language,” in *2023 IEEE/CVF Conference on Computer Vision and Pattern Recognition (CVPR)*, 2023, pp. 15 116–15 127.
- [20] F. Liang, B. Wu, X. Dai *et al.*, “Open-vocabulary semantic segmentation with mask-adapted clip,” in *Proceedings of the IEEE/CVF Conference on Computer Vision and Pattern Recognition*, 2023, pp. 7061–7070.
- [21] C. Huang, O. Mees, A. Zeng, and W. Burgard, “Visual language maps for robot navigation,” in *Proceedings of the IEEE International Conference on Robotics and Automation (ICRA)*, 2023.
- [22] B. Chen, F. Xia, B. Ichter, K. Rao, K. Gopalakrishnan, M. S. Ryoo, A. Stone, and D. Kappler, “Open-vocabulary queryable scene representations for real world planning,” in *Proceedings of the IEEE International Conference on Robotics and Automation (ICRA)*, 2023.
- [23] H. Ha and S. Song, “Semantic abstraction: Open-world 3D scene understanding from 2D vision-language models,” in *Proceedings of the 2022 Conference on Robot Learning (CoRL)*, 2022.
- [24] S. Peng, K. Genova, C. Jiang, A. Tagliasacchi, M. Pollefeys, and T. Funkhouser, “Openscene: 3d scene understanding with open vocabularies,” in *Proceedings of the IEEE/CVF Conference on Computer Vision and Pattern Recognition (CVPR)*, 2023.
- [25] K. Jatavallabhula, A. Kuwajerwala, Q. Gu *et al.*, “Conceptfusion: Open-set multimodal 3d mapping,” in *Proceedings of the Robotics: Science and System (RSS)*, 2023.
- [26] N. Muhammad, C. Paxton, L. Pinto, S. Chintala, and A. Szlam, “Clip-fields: Weakly supervised semantic fields for robotic memory,” in *Proceedings of the Robotics: Science and System (RSS)*, 2023.
- [27] T. P. McNamara, J. K. Hardy, and S. C. Hirtle, “Subjective hierarchies in spatial memory,” *Journal of experimental psychology: Learning, memory, and cognition*, vol. 15 2, pp. 211–27, 1989.
- [28] A. J. Davison, “Futuremapping: The computational structure of spatial ai systems,” in *arXiv preprint arXiv:1803.11288*, 2018.
- [29] F. Xia, A. R. Zamir, Z. He *et al.*, “Gibson env: Real-world perception for embodied agents,” in *Conference on Computer Vision and Pattern Recognition (CVPR)*, 2018, pp. 9068–9079.
- [30] K. Chen, J. K. Chen, J. Chuang, M. Vázquez, and S. Savarese, “Topological planning with transformers for vision-and-language navigation,” in *2021 IEEE/CVF Conference on Computer Vision and Pattern Recognition (CVPR)*, 2021, pp. 11 271–11 281.
- [31] I. Armeni, Z.-Y. He, J. Gwak, A. R. Zamir, M. Fischer, J. Malik, and S. Savarese, “3d scene graph: A structure for unified semantics, 3d space, and camera,” in *Proceedings of the IEEE/CVF International Conference on Computer Vision (ICCV)*, October 2019.
- [32] R. Karlsson, A. Carballo, K. Fujii, K. Ohtani, and K. Takeda, “Predictive world models from real-world partial observations,” in *IEEE International Conference on Mobility, Operations, Services and Technologies (MOST)*, 2023, pp. 152–166.
- [33] L. ling Wu and L. W. Barsalou, “Perceptual simulation in conceptual combination: Evidence from property generation,” *Acta Psychologica*, vol. 132, no. 2, pp. 173–189, 2009.
- [34] L. W. Barsalou, *The Human Conceptual System*, ser. Cambridge Handbooks in Psychology. Cambridge University Press, 2012, p. 239–258.
- [35] M. Eysenck and M. Keane, *Cognitive Psychology: A Student’s Handbook - 8th ed.* Psychology Press, 2020.
- [36] J. Lambert, Z. Liu, O. Sener, J. Hays, and V. Koltun, “Mseg: A composite dataset for multi-domain semantic segmentation,” in *2020 IEEE/CVF Conference on Computer Vision and Pattern Recognition (CVPR)*, 2020, pp. 2876–2885.
- [37] E. Rosch, C. B. Mervis, W. D. Gray, D. M. Johnson, and P. Boyes-Braem, “Basic objects in natural categories,” *Cognitive Psychology*, vol. 8, no. 3, pp. 382–439, 1976.
- [38] J. R. Binder and R. H. Desai, “The neurobiology of semantic memory,” *Trends in Cognitive Sciences*, vol. 15, no. 11, pp. 527–536, 2011.
- [39] M. R. Quillian, “A design for an understanding machine,” Paper presented at a colloquium: Semantic Problems in Natural Language, King’s College, Cambridge, England, Sep 1961.
- [40] W. V. O. Quine, *From a Logical Point of View*. Harvard University Press, 1953.
- [41] L. Wittgenstein, *Philosophical Investigations*. Blackwell Publishing, Inc., 1953.
- [42] G. Lakoff, *Women, Fire, and Dangerous Things*. University of Chicago Press, 1987.
- [43] I. Schwartz, *Naming, Necessity, and Natural Kinds*. Cornell University Press, 1977.
- [44] S. J. Russel and P. Norvig, *Artificial Intelligence: A Modern Approach*, 4th ed. Prentice Hall, 2020.
- [45] J. McCarthy, “Programs with common sense,” in *Proc. Symposium on Mechanisation of Thought Processes*, vol. 1, 1958, pp. 77–84.
- [46] L. A. Zadeh, “Fuzzy sets,” *Information and Control*, vol. 8, pp. 338–353, 1965.
- [47] S. A. Kripke, “A completeness theorem in modal logic,” *Journal of Symbolic Logic*, vol. 24, pp. 1 – 14, 1959.
- [48] M. L. Minsky, “A framework for representing knowledge,” in *The Psychology of Computer Vision*. McGraw-Hill, 1975, pp. 211–277.
- [49] J. Devlin, M.-W. Chang, K. Lee, and K. Toutanova, “BERT: Pre-training of deep bidirectional transformers for language understanding,” in *Proceedings of the 2019 Conference of the North American Chapter of the Association for Computational Linguistics*, 2019, pp. 4171–4186.
- [50] N. Reimers and I. Gurevych, “Sentence-bert: Sentence embeddings using siamese bert-networks,” in *Proceedings of the 2019 Conference on Empirical Methods in Natural Language Processing (EMNLP)*, 2019.
- [51] T. Mikolov, I. Sutskever, K. Chen, G. Corrado, and J. Dean, “Distributed representations of words and phrases and their compositionality,” in *Advances in Neural Information Processing Systems (NIPS)*, 2013.
- [52] J. Pennington, R. Socher, and C. D. Manning, “Glove: Global vectors for word representation,” in *Conference on Empirical Methods in Natural Language Processing (EMNLP)*, 2014.
- [53] S. Harris, “Distributional structure,” *WORD*, vol. 10, pp. 146–162, 1954.
- [54] M. E. Peters, M. Neumann, M. Iyyer, M. Gardner, C. Clark, K. Lee, and L. Zettlemoyer, “Deep contextualized word representations,” in *Proceedings of the Conference of the North American Chapter of the Association for Computational Linguistics*, 2018, pp. 2227–2237.
- [55] Q. Le and T. Mikolov, “Distributed representations of sentences and documents,” in *Proceedings of the 31st International Conference on Machine Learning*, vol. 32, no. 2. PMLR, 2014, pp. 1188–1196.
- [56] A. Maas and A. Ng, “A probabilistic model for semantic word vectors,” in *Advances in Neural Information Processing Systems (NIPS)*, 2010.
- [57] D. M. Blei, A. Y. Ng, and M. I. Jordan, “Latent dirichlet allocation,” *Journal of Machine Learning Research*, vol. 3, pp. 993–1022, 2003.

- [58] M. Hoffman, F. Bach, and D. Blei, "Online learning for latent dirichlet allocation," in *Adv. in Neural Information Processing Systems*, 2010.
- [59] J. Li, D. Li, S. Savarese, and S. C. H. Hoi, "Blip-2: Bootstrapping language-image pre-training with frozen image encoders and large language models," in *arXiv preprint arXiv:2203.03897*, 2023.
- [60] H. Liu, C. Li, Q. Wu, and Y. J. Lee, "Visual instruction tuning," in *arXiv preprint arXiv:2304.08485*, 2023.
- [61] B. Cheng, I. Misra, A. Schwing, A. Kirillov, and R. Girdhar, "Masked-attention mask transformer for universal image segmentation," *IEEE/CVF Conference on Computer Vision and Pattern Recognition (CVPR)*, 2022.
- [62] Y. Zhong, J. Yang, P. Zhang *et al.*, "Regionclip: Region-based language-image pretraining," in *IEEE/CVF Conference on Computer Vision and Pattern Recognition*, 2022, pp. 16 793–16 803.
- [63] J. Kerr, C. M. Kim, K. Goldberg, A. Kanazawa, and M. Tancik, "Lerf: Language embedded radiance fields," in *International Conference on Computer Vision (ICCV)*, 2023.
- [64] B. Mildenhall, P. P. Srinivasan, M. Tancik, J. T. Barron, R. Ramamoorthi, and R. Ng, "Nerf: Representing scenes as neural radiance fields for view synthesis," in *ECCV*, 2020.
- [65] X. Gu, T.-Y. Lin, W. Kuo, and Y. Cui, "Open-vocabulary object detection via vision and language knowledge distillation," in *International Conference on Learning Representations (ICLR)*, 2022.
- [66] J. Ding, N. Xue, G.-S. Xia, and D. Dai, "Decoupling zero-shot semantic segmentation," in *IEEE Conference on Computer Vision and Pattern Recognition (CVPR)*, 2022.
- [67] T. Lüddecke and A. Ecker, "Image segmentation using text and image prompts," in *Proceedings of the IEEE/CVF Conference on Computer Vision and Pattern Recognition (CVPR)*, June 2022, pp. 7086–7096.
- [68] S. Thrun, M. Montemerlo, H. Dahlkamp *et al.*, "Stanley: The robot that won the darpa grand challenge," *Journal of Field Robotics*, vol. 23, no. 9, pp. 661–692, 2006.
- [69] P. Besl and N. D. McKay, "A method for registration of 3-d shapes," *IEEE Transactions on Pattern Analysis and Machine Intelligence*, vol. 14, no. 2, pp. 239–256, 1992.
- [70] R. Smith and P. Cheeseman, "On the representation and estimation of spatial uncertainty," *The Int. J. of Robotics Research*, vol. 5, no. 4, 1986.
- [71] M. Labbé and F. Michaud, "Rtab-map as an open-source lidar and visual simultaneous localization and mapping library for large-scale and long-term online operation," *Journal of Field Robotics*, vol. 36, no. 2, pp. 416–446, 2019.
- [72] K. M. Jatavallabhula, G. Iyer, and L. Paull, "∇slam: Dense slam meets automatic differentiation," in *2020 IEEE International Conference on Robotics and Automation (ICRA)*, 2020, pp. 2130–2137.
- [73] I. Vizzo, T. Guadagnino, B. Mersch, L. Wiesmann, J. Behley, and S. Cyrill, "KISS-ICP: In Defense of Point-to-Point ICP Simple, Accurate, and Robust Registration If Done the Right Way," *IEEE Robotics and Automation Letters (RA-L)*, vol. 8, no. 2, pp. 1029–1036, 2023.
- [74] R. F. Salas-Moreno, R. A. Newcombe, H. Strasdat, P. H. Kelly, and A. J. Davison, "Slam++: Simultaneous localisation and mapping at the level of objects," in *IEEE Conference on Computer Vision and Pattern Recognition (CVPR)*, 2013, pp. 1352–1359.
- [75] J. McCormac, A. Handa, A. Davison, and S. Leutenegger, "SemanticFusion: Dense 3d semantic mapping with convolutional neural networks," in *Int. Conf. on Robotics and Automation (ICRA)*, 2017, pp. 4628–4635.
- [76] S. Schuster, M. Zhai, N. Jacobs, and M. Chandraker, "Learning to look around objects for top-view representations of outdoor scenes," in *European Conference on Computer Vision (ECCV)*, 2018, pp. 815–831.
- [77] J. Ost, F. Mannan, N. Thuerey, J. Knodt, and F. Heide, "Neural scene graphs for dynamic scenes," in *IEEE Conference on Computer Vision and Pattern Recognition (CVPR)*, June 2021, pp. 2856–2865.
- [78] R. Martin-Brualla, N. Radwan, M. S. M. Sajjadi, J. T. Barron, A. Dosovitskiy, and D. Duckworth, "NeRF in the Wild: Neural Radiance Fields for Unconstrained Photo Collections," in *IEEE Conference on Computer Vision and Pattern Recognition (CVPR)*, 2021.
- [79] R. Pi, J. Gao, S. Diao *et al.*, "Detgpt: Detect what you need via reasoning," in *arXiv preprint arXiv:2305.14167*, 2023.
- [80] J. J. Gibson, "The ecological approach to visual perception," in *Houghton, Mifflin and Company*, 1979.
- [81] A. Milner and M. Goodale, "Two visual systems re-viewed," *Neuropsychologia*, vol. 46, no. 3, pp. 774–785, 2008, consciousness and Perception: Insights and Hindsight.
- [82] Z. Han and A. Sereno, "Modeling the ventral and dorsal cortical visual pathways using artificial neural networks," *Neural Computation*, vol. 34, no. 1, pp. 138–171, 2022.
- [83] T. M. Janssen and B. H. Partee, "Chapter 7 - compositionality," in *Handbook of Logic and Language*. North-Holland, 1997, pp. 417–473.
- [84] R. Vershynin, *High-Dimensional Probability: An Introduction with Applications in Data Science*. Cambridge University Press, 2018.
- [85] J. So, C. Oh, Y. Lim, H. Byun, M. Shin, and K. Song, "Geodesic multi-modal mixup for robust fine-tuning," in *arXiv:2203.03897*, 2022.
- [86] F. Wang and H. Liu, "Understanding the behaviour of contrastive loss," in *2021 IEEE/CVF Conference on Computer Vision and Pattern Recognition (CVPR)*, 2021, pp. 2495–2504.
- [87] A. Dosovitskiy, L. Beyer, A. Kolesnikov *et al.*, "An image is worth 16x16 words: Transformers for image recognition at scale," in *International Conference on Learning Representations (ICLR)*, 2021.
- [88] Z. Chen, Y. Duan, W. Wang, J. He, T. Lu, J. Dai, and Y. Qiao, "Vision transformer adapter for dense predictions," in *International Conference on Learning Representations (ICLR)*, 2023.
- [89] T.-Y. Lin, P. Dollár, R. Girshick, K. He, B. Hariharan, and S. Belongie, "Feature pyramid networks for object detection," in *IEEE Conference on Computer Vision and Pattern Recognition (CVPR)*, 2017, pp. 936–944.
- [90] Z. Cui, W. Longshi, and R. Wang, "Open set semantic segmentation with statistical test and adaptive threshold," in *IEEE International Conference on Multimedia and Expo (ICME)*, 2020, pp. 1–6.
- [91] G. A. Miller, "Wordnet: A lexical database for english," *Communications of the ACM*, vol. 38, no. 11, p. 39–41, Nov 1995.
- [92] H. Caesar, J. Uijlings, and V. Ferrari, "Coco-stuff: Thing and stuff classes in context," in *2018 IEEE/CVF Conference on Computer Vision and Pattern Recognition*, 2018, pp. 1209–1218.
- [93] A. Kirillov, E. Mintun, N. Ravi *et al.*, "Segment anything," *arXiv:2304.02643*, 2023.
- [94] H. Bao, L. Dong, S. Piao, and F. Wei, "BEiT: BERT pre-training of image transformers," in *Int. Conf. on Learning Representations*, 2022.
- [95] K. He, X. Zhang, S. Ren, and J. Sun, "Deep residual learning for image recognition," in *2016 IEEE Conference on Computer Vision and Pattern Recognition (CVPR)*, 2016, pp. 770–778.
- [96] S. Li, "Concise formulas for the area and volume of a hyperspherical cap," *Asian Journal of Mathematics & Statistics*, vol. 4, pp. 66–70, 2011.
- [97] T. Wang and P. Isola, "Understanding contrastive representation learning through alignment and uniformity on the hypersphere," in *International Conference on Machine Learning (ICML)*, 2020, pp. 9929–9939.
- [98] M. P. Deisenroth, A. A. Faisal, and C. S. Ong, *Mathematics for Machine Learning*. Cambridge University Press, 2020.
- [99] S. Boyd and L. Vandenberghe, *Convex Optimization*. Cambridge University Press, 2004.

Robin Karlsson (Student Member, IEEE) received a BSc. degree from the School of Engineering, Aalto University, Finland, and an MSc. degree from the Graduate School of Frontier Science, University of Tokyo, Japan. From 2018 to 2021 he worked as an autonomous vehicle research scientist at Ascent Robotics and TIER IV. He is currently pursuing a Ph.D. degree at the Graduate School of Informatics, Nagoya University, Japan. His research interest includes neurosymbolic AI, world representations for general-purpose mobile robotics, machine reasoning, and AGI. His contributions include two international conference best paper awards, a national student competition 1st place, and the IEEE ITSS Young Researcher Award.

Francisco Lepe-Salazar pursued his graduate studies at Waseda University, Japan. He is currently the Managing Director of Ludolab, the Director of the Observatorio Nacional de la Industria de los Videojuegos with DevsVJ MX, a Creator and an Organizer with International Contest Games4Empowerment, a Founding Member of the Educational Program Código Frida, and a Teacher with the University of Colima, Mexico, and the Deggendorf Institute of Technology, Germany. His research interests include cognitive science, human-computer interaction, and user empowerment. His contributions include various publications at top international venues.

Kazuya Takeda (Governors member, IEEE ITS Society; Governors member, APSIPA; Fellow, IEICE) serves as a Vice President of Nagoya University and Professor at Nagoya University's Institute of Innovation for Future Society and Graduate School of Informatics. He is also a Director at Tier IV, Inc. Dr. Takeda earned his Bachelor's, Master's, and Ph.D. from Nagoya University in 1983, 1985, and 1993, respectively. He has held positions at ATR (Advanced Telecommunication Research Laboratories) and KDD R&D Lab, in addition to being a visiting scientist at MIT. His research primarily focuses on signal processing and machine learning of behavior signals and their applications. With over 150 journal papers, 9 co-authored/co-edited books, and 15 patents to his name, Dr. Takeda is a prolific contributor to his field. His achievements include the 2020 IEEE ITS Society Outstanding Research Award and six best paper awards from IEEE international conferences and workshops, in addition to various domestic awards.